

**AD 664956**

Technical Report

**R 564**

DASA-RSS3318

**MIX DESIGN FOR SMALL-SCALE MODELS  
OF CONCRETE STRUCTURES**

February 1968

NAVAL FACILITIES ENGINEERING COMMAND



NAVAL CIVIL ENGINEERING LABORATORY

Port Hueneme, California

This document has been approved for public  
release and sale; its distribution is unlimited.

FEB 14 1968

Reproduced by the  
**CLEARINGHOUSE**  
for Federal Scientific & Technical  
Information Springfield Va. 22151

71

## CONTENTS

	page
INTRODUCTION .....	1
Objective .....	1
Definitions .....	1
Previous Work .....	2
SCOPE AND APPROACH .....	3
EXPERIMENTAL TECHNIQUES .....	5
Materials .....	5
Forms .....	6
Mixing .....	11
Casting .....	12
Curing .....	13
Capping .....	14
Testing .....	14
RESULTS AND DISCUSSION .....	19
Workability .....	19
Compressive Strength Versus Age .....	20
Compressive Strength Versus Water-Cement Ratio .....	23
Splitting Tensile Strength .....	30
Flexural Strength of Concretes .....	36
Flexural Strength of Hollow Beams .....	40
Stress-Strain Relation in Compression .....	42
Effect of Specimen Size on Strength .....	46
MIX DESIGN PROCEDURE AND EXAMPLES .....	49

	page
Design Procedure .....	49
Mix Design Examples .....	51
EVALUATION OF MIX DESIGN PROCEDURE .....	56
CONCLUSIONS .....	58
ACKNOWLEDGMENTS .....	58
APPENDIX – Comparison of Ultracal 30 and Hydro-stone as Cementing Agents for Gypsum Concrete .....	60
LIST OF SYMBOLS .....	63
REFERENCES .....	65

## INTRODUCTION

### Objective

In recent years interest has grown in the use of small-scale direct models in structural engineering research and design. To further the development of modeling techniques, a research project was initiated at the Naval Civil Engineering Laboratory (NCEL) under the sponsorship of the Defense Atomic Support Agency (DASA). The primary objective of the first phase of this project was to develop a mix design procedure for the concretes used in small-scale direct models of concrete structures. A secondary objective was to gain experience in, and improve techniques for, the manufacture and testing of small-sized concrete specimens.

### Definitions

**Direct Model.** A direct model is geometrically similar to the prototype structure. Under similar loading patterns, the strain distribution in the model and prototype are identical, and nonlinear geometrical effects in the prototype are reproduced in the model. A direct model can be one of two types, either elastic or inelastic. The former is useful in studying the elastic behavior of a structure; the latter is useful in studying the behavior up to and including failure. The direct inelastic model of a concrete structure should reproduce the effects of the nonlinear stress-strain relation and tensile cracking of concrete, as well as the effects of yielding or fracture of reinforcing steel.

**Small Scale.** Small-scale models are of tabletop size and have beam and column cross-sectional dimensions of about 1-1/2 inches or less and slab and shell thicknesses of about 1/4 inch or less. In the case of a direct inelastic model of a concrete structure, small-scale implies a scaling down of the prototype materials. For example, deformed reinforcing bars of sufficiently small diameter are not available for the model, and the particle sizes of coarse aggregate are too large to be compatible with the dimensions of the model.

**Prototype Concrete.** For this report, prototype concrete is defined as portland cement concrete made with normal-weight aggregate having a maximum size of 1/2 inch or greater. The strength properties of prototype

concrete are determined by testing standard-size specimens at an age of 7 days or greater using the methods specified by the American Society for Testing and Materials (ASTM). Where no confusion results, prototype concrete will be referred to as concrete.

**Microconcrete.** Microconcrete is a mixture of suitably graded sand, portland cement, and water used to simulate concrete in small-scale models.

**Gypsum Concrete.** Gypsum concrete is a mixture of suitably graded sand, high-strength gypsum cement, and water used to simulate concrete in small-scale models.

**Model Concrete.** Model concrete is microconcrete or gypsum concrete. Where no confusion results, model concrete will be referred to as concrete.

### Previous Work

In the last 50 years or so, indirect and direct elastic modeling techniques have been highly developed and used successfully in many research and design studies. During the last 15 years or so, the growth of interest in plastic design, ultimate-strength design, and limit design of statically and dynamically loaded structures has resulted in increased emphasis on the development of direct inelastic modeling techniques. Most of the technical literature concerning the development of these techniques for concrete structures has been listed and categorized in Reference 1.

In the direct inelastic model studies of structural behavior which have been carried out in this country in the past, microconcrete has usually been used as the substitute for concrete. In Europe and Australia, however, extensive use has been made of various gypsum cementing agents, usually combined only with water, to simulate concrete. The advantage of the gypsum-based model concretes over microconcrete, of course, is the rapid rate of strength development, which, in some cases, allows a model to be tested on the day of casting. To capitalize on this advantage, gypsum concrete has been used in some of the more recent model studies<sup>2,3</sup> in this country.

Specific examples of mix designs for small-scale concrete models are given in many of the publications listed in Reference 1; several examples can be found in References 3 and 4. Mix design methods intended specifically for microconcrete have been outlined in References 3 and 5. The first step in the method described in Reference 3 is to specify (1) the compressive strength,  $f'_c$ ; (2) secant modulus to, for example, 45%  $f'_c$ ; and (3) compressive strain at a stress of, for example, 95%  $f'_c$  to make the microconcrete represent a particular prototype concrete. Then, the water-cement ratio and volume of

aggregate approximately satisfying the specified properties are chosen from a set of curves. Reference 3 indicates that only rarely has it been found possible to satisfy simultaneously the three specified properties and still have a workable mixture. In this method, experience must be relied upon to determine if a particular mix will be workable. In the method described in Reference 5, the water-cement ratio and aggregate-cement ratio are related by a criterion of workability. After specifying the desired compressive strength of the microconcrete, the water-cement ratio is chosen from a set of curves. The properties of the microconcrete stress-strain curve are not specified; hence, one must accept the stress-strain curve produced by the chosen water-cement ratio and its accompanying aggregate-cement ratio.

### SCOPE AND APPROACH

The method of mix design proposed in Reference 5 and described briefly in the previous section was adopted for this study. Sufficient data were accumulated to define the workability (aggregate-cement ratio versus water-cement ratio) curves for a variety of maximum aggregate sizes in both microconcrete and gypsum concrete. After studying the development of compressive strength with age and determining the most desirable age for testing, data were collected to define the  $f'_c$  versus water-cement ratio curves for both microconcrete and gypsum concrete having No. 4 and No. 30 maximum aggregate. Several of the considerations involved in choosing (1) the aggregate sizes to concentrate most effort upon, (2) the auxiliary tests to perform, and (3) the test specimen sizes and experimental techniques to use are discussed in the following paragraphs.

A survey of recent research on reinforced concrete structural elements showed that the most commonly used ratio of maximum aggregate size to minimum member dimension was 1:8 for beams and columns and 1:5 for slabs and shells. A ratio of about 1:8 was chosen for use in all small-scale models. Then, if the typical model beam or column dimension is 1-1/2 inches and the typical slab or shell thickness is 1/4 inch, the corresponding maximum aggregate sizes will be No. 4 and No. 30. As mentioned above, the  $f'_c$  versus water-cement ratio curves were developed for model concretes having these two aggregate sizes only. It was felt that the strength of concretes with other aggregate sizes could be found with sufficient accuracy by interpolating between the curves for the No. 4 and No. 30 sizes.

In the method of mix design adopted for this study, the compressive strength is the only material property to be specified. To obtain the best predictions of prototype behavior from the results of model tests, the other

material properties of the model concrete should be similar to those of a prototype concrete having the same compressive strength. Therefore, tests were performed to determine the splitting tensile strength, flexural strength, and compressive stress-strain curve of some of the model concretes. The results of these tests were compared with the results from similar tests on prototype concrete.

In determining the strengths of model concretes, a decision is necessary about the size of specimen to test because the indicated compressive, splitting tensile, and flexural strengths of a particular model concrete tested at a given age are often observed to increase with decreasing absolute size of the test specimen.<sup>3,4,5</sup> There are at least three possible approaches to choosing the test specimen size:

1. Establish standard specimen sizes (possibly 1 x 2-inch cylinders and 1 x 1 x 3-inch beams) for model concretes, an approach similar to the practice used in testing prototype concrete (6 x 12-inch cylinders and 6 x 6 x 18-inch beams).
2. Scale down the standard prototype-concrete test cylinders in accordance with the scale of the model being tested. For example, 1/2 x 1-inch cylinders would be tested with a 1/42-scale model. This approach requires the designation of a specific prototype structure, which is not always possible or desirable when models are used in research studies.
3. Use specimen cross-sectional dimensions approximately the same as typical cross-sectional dimensions of the model. For example, 1 x 2-inch cylinders would be used with a model having 1-inch-square columns.

There is presently insufficient knowledge, from either experiment or theory, to determine which of the three approaches should be used. It is noted that a new technique of scaling gypsum concrete specimens<sup>3</sup> promises to nearly eliminate the so-called size effect, thereby making less critical the choice of test specimen size.

In most of this investigation, test specimen sizes were chosen in accordance with the third approach outlined above; each specimen had a diameter or wall thickness approximately the same as a typical cross-sectional dimension of the model in which the concrete being tested would be used. When this approach and the approach outlined above for determining the maximum aggregate size are used, the applicable dimension (diameter or wall thickness of a hollow sphere) of the test specimen becomes about 8 times the aggregate size.

During the course of the work, emphasis was placed on using and developing experimental techniques that would be easy to apply and would produce valid, repeatable results. In general, the testing techniques were scaled-down (where necessary) versions of standard ASTM tests, and the forming and casting techniques were patterned after the techniques described in References 3 and 4. The age at testing for gypsum concrete and the curing procedure for microconcrete differed somewhat from those used by other investigators. The curing procedure and test age were changed to allow time for application of strain gages and setting up the test before the testing of a model structure. In another departure from previously used techniques, hollow cylinders were used and hollow beams were investigated for determining the compressive and tensile strengths, respectively, of the concretes having No. 30 aggregate. This was done because of the difficulty of casting and testing, and the variability of the results from using extremely small (1/4 x 1/2-inch) solid cylinders.

Experimental techniques are outlined in detail in the next section of the report. In subsequent sections, test results are presented and discussed, several mix design examples are shown, and conclusions are drawn about the experimental techniques and the properties of the model concretes.

## EXPERIMENTAL TECHNIQUES

### Materials

**Cements.** Type III (high early strength) portland cement (Velo) manufactured by Monolith Portland Cement Company was used in all the microconcretes. For the gypsum concretes discussed in the main body of the report, Ultracal 30, manufactured by the U. S. Gypsum Company, was used as the cementing agent. Hydro-stone, also manufactured by the U. S. Gypsum Company, was used in some gypsum concretes, yielding the results presented in the Appendix. Another potentially useful gypsum cement is Ultracal 60, which has a longer time-to-set than does Ultracal 30 or Hydro-stone. Table 1 shows typical physical data furnished by the manufacturer for the three gypsum cements.

**Aggregate.** San Gabriel River wash sand and gravel, obtained near Irwindale, California, was used in all the concretes. This aggregate is composed chiefly of granitic feldspar and quartz particles, with some biotite, hornblende and magnetite in the fine sizes.<sup>6</sup> The sand particles are subangular and angular in shape with a moderately rough surface texture.

Table 1. Physical Data for Concretes Made With Gypsum Cements<sup>1/</sup>

Cement	Water-Cement Ratio for Normal Consistency <sup>2/</sup> Concrete (by weight)	Normal Setting Time (min)	Typical Setting Expansion (in./in.)	Average Compressive Strength, Dry <sup>3/</sup> (psi)
Ultracal 30	0.35-0.38	25-35	0.0003	7,300
Ultracal 60	0.36-0.39	75-90	0.0002	7,300
Hydro-stone	0.28-0.32	20-25	0.002	11,000

<sup>1/</sup>Taken from U. S. Gypsum Company Bulletin IGL-116, March 1965.

<sup>2/</sup>Consistency to make a pourable slurry.

<sup>3/</sup>Dried to constant weight at 110°F. Wet strength is about one-half the dry strength.

The aggregate was oven-dried, separated into fractions (U. S. Sieve Series:), and then stored in nearly moisture-tight containers. The moisture content when the aggregate was used, specific gravity, and absorption for each fraction are shown in Table 2. When used to make the model concretes, the aggregate fractions were combined in the proportions listed in Table 3 to form the gradation curves shown in Figure 1. The gradation curves were developed initially by choosing an S-shaped curve for the 3/8-inch maximum size aggregate and then successively eliminating the coarsest fraction to obtain the curves for successively smaller maximum aggregate sizes.

#### Forms

All specimens were cast in specially constructed plexiglass forms. Plexiglass was used because it machines easily; remains flexible and transparent; provides a smooth, hard surface; and is easy to clean. Figures 2, 3, and 4 show typical cylinder and beam forms.

Table 2. Properties of San Gabriel Aggregate

Fraction		Moisture Content (%)	Specific Gravity (ovendry)	Absorption (%)
Smaller Than	Larger Than			
3/8 in.	No. 4	0.3	2.69	0.9
No. 4	No. 8	0.3	2.66	1.0
No. 8	No. 16	0.3	2.67	1.1
No. 16	No. 30	0.2	2.67	2.5
No. 30	No. 50	0.3	2.74	—
No. 50	No. 100	0.3	2.65	—
No. 100	Pan	0.4	2.61	—

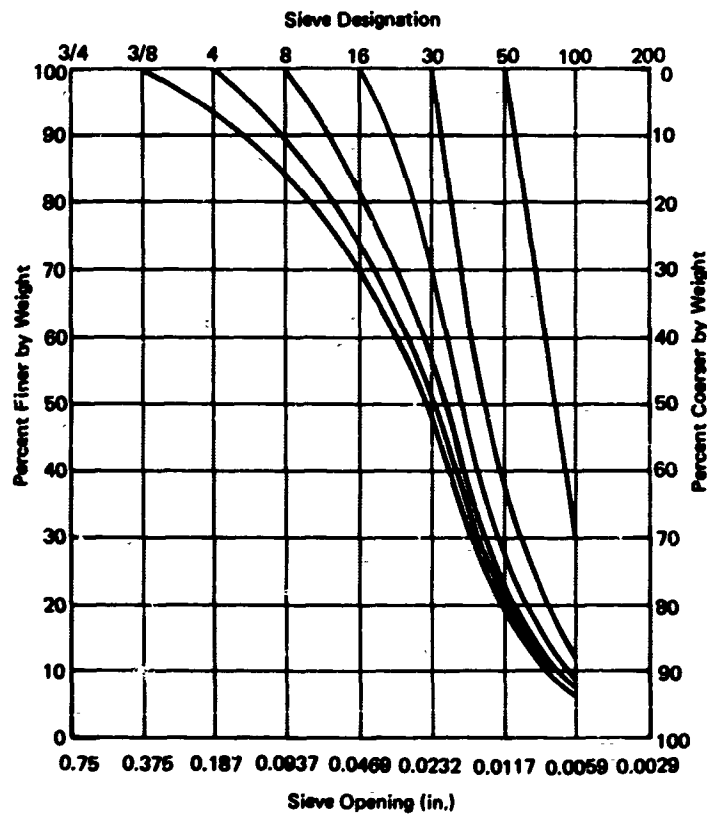


Figure 1. Aggregate gradations used in model concretes.

Table 3. Aggregate Gradations for Model Concretes

Maximum Aggregate Size	Fraction		Percentage by Weight	Cumulative Percentage
	Smaller Than	Larger Than		
3/8 in.	3/8 in.	No. 4	6	6
	No. 4	No. 8	9	15
	No. 8	No. 16	15	30
	No. 16	No. 30	21	51
	No. 30	No. 50	30	81
	No. 50	No. 100	13	94
	No. 100	Pan	6	100
No. 4	No. 4	No. 8	10	10
	No. 8	No. 16	15	25
	No. 16	No. 30	23	48
	No. 30	No. 50	32	80
	No. 50	No. 100	14	94
	No. 100	Pan	6	100
No. 8	No. 8	No. 16	18	18
	No. 16	No. 30	24	42
	No. 30	No. 50	36	78
	No. 50	No. 100	15	93
	No. 100	Pan	7	100
No. 16	No. 16	No. 30	30	30
	No. 30	No. 50	43	73
	No. 50	No. 100	18	91
	No. 100	Pan	9	100
No. 30	No. 30	No. 50	61	61
	No. 50	No. 100	27	88
	No. 100	Pan	12	100
No. 50	No. 50	No. 100	68	68
	No. 100	Pan	32	100

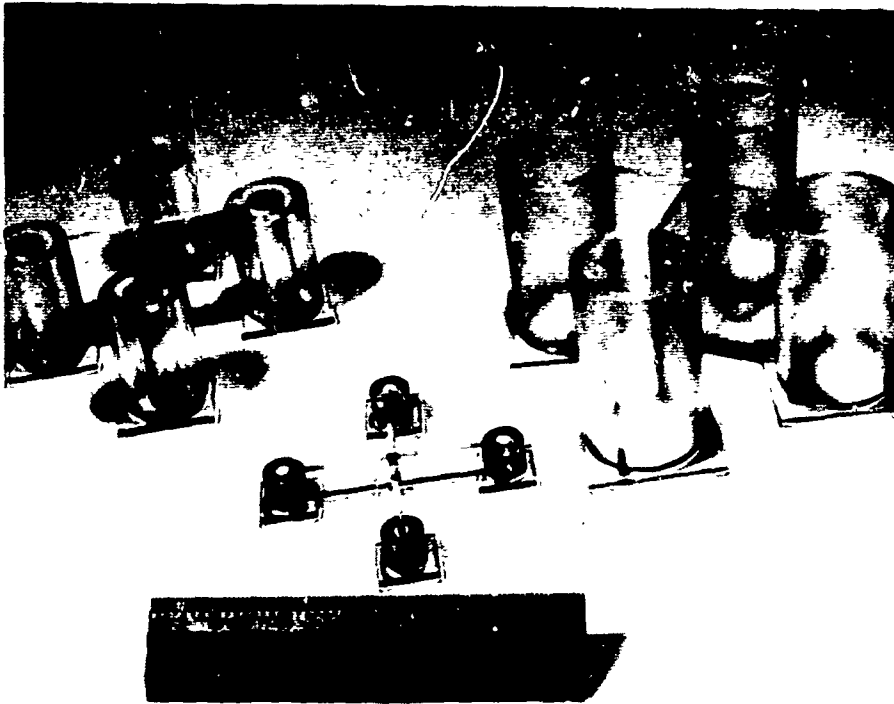


Figure 2. Plexiglass forms for cylindrical specimens.

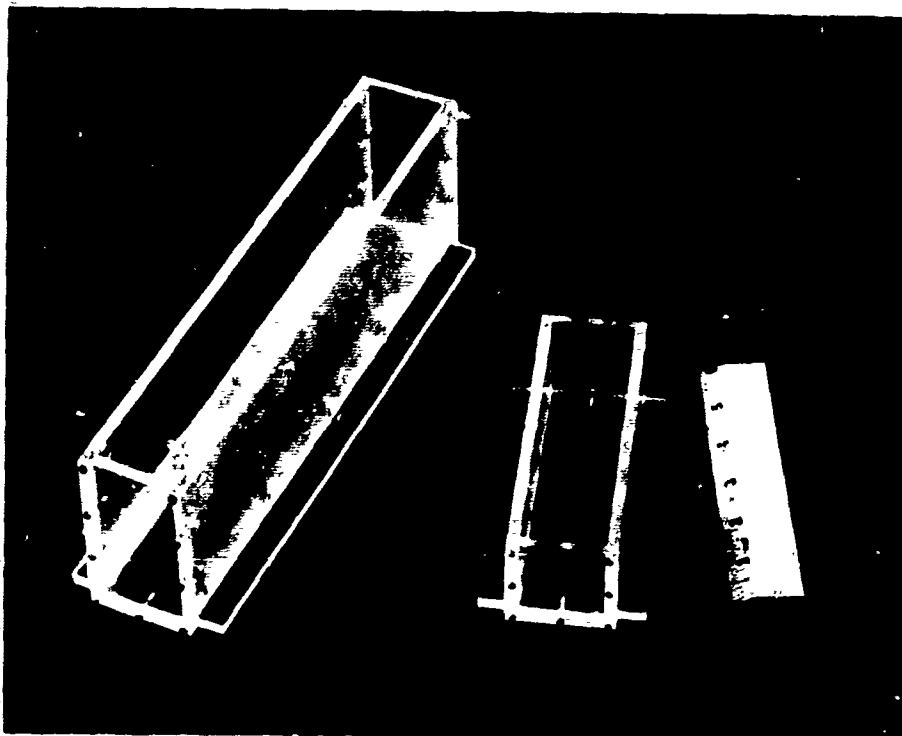


Figure 3. Forms for two sizes of beams.

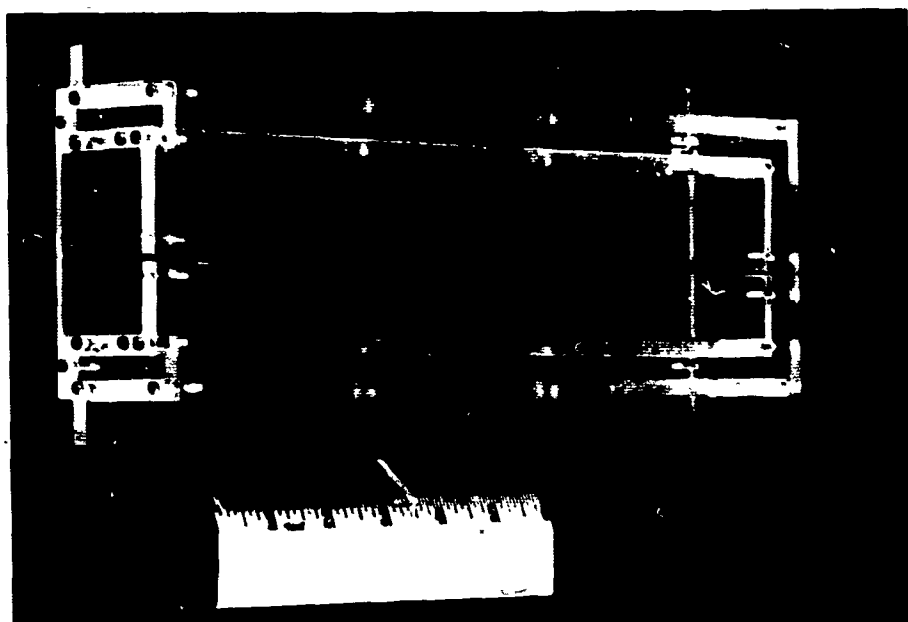


Figure 4. Form for one-half of a hollow beam.

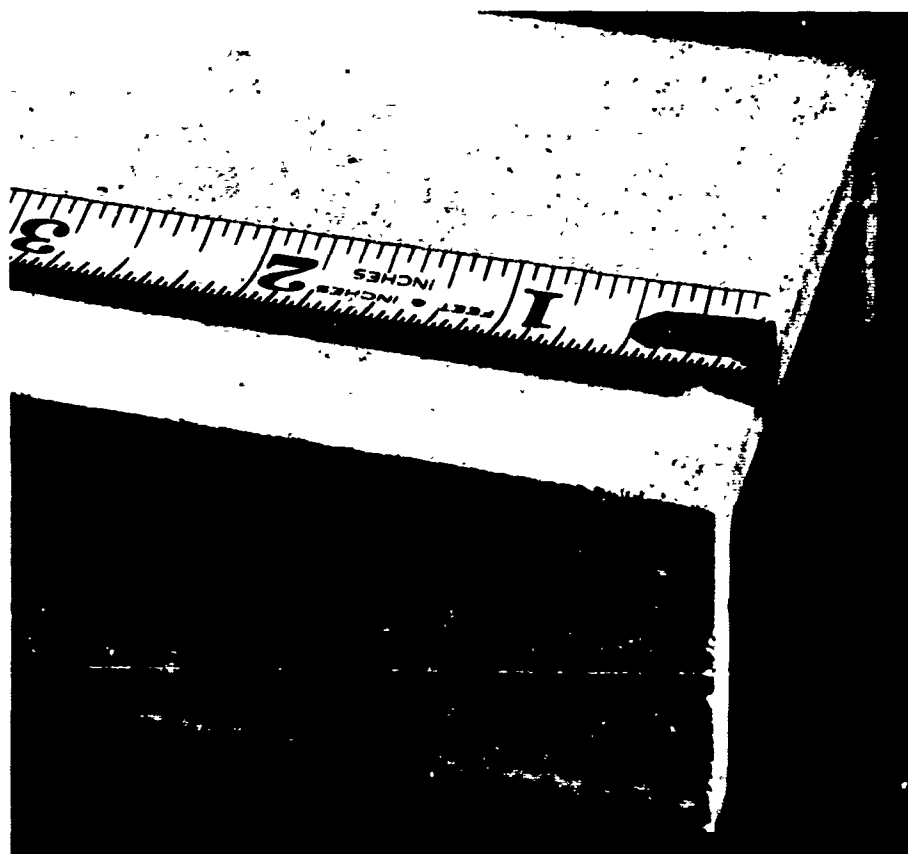


Figure 5. View of portion of one-half of a hollow beam.

The forms for solid cylinders (Figure 2) were fabricated by center-boring plexiglass rods of appropriate diameters to a wall thickness of 3/16 inch. Then a 1/16-inch-wide slit was made along the length of the form to provide a means for spreading the form to remove the test cylinder after casting. A plexiglass strip was inserted in the slit to prevent leakage during casting.

A typical cluster of hollow-cylinder forms is shown in the upper left corner of Figure 2. Each form consisted of a slightly tapered plexiglass rod, which was inserted in the cylinder and fastened with a screw to the bottom plate.

The beam forms shown in Figure 3 were fabricated from 1/4-inch-thick plexiglass sheets. The forms were provided with a protruding base plate so that the forms could be clamped down during vibration of the concrete.

Figure 4 shows the form for one-half of a 1/4-inch-thick hollow beam. The top plate of this form was slit longitudinally to aid in removing the plate from the finished casting. The slit was filled during casting by a vertically placed strip of plexiglass. A portion of a finished casting from the hollow beam form is shown in Figure 5.

To prepare the forms for casting, a light coating of silicone grease was applied to both the inside and outside of each component of the form to reduce the adhesion of the concrete. Finally, the forms were assembled with No. 2-56 slotted steel machine screws and checked for tightness of joints.

### Mixing

Both microconcrete and gypsum concrete were mixed in one of two planetary action, laboratory-sized mixers. For batches larger than 120 in.<sup>3</sup>, a 20-quart-capacity Blakeslee Mixer was used; for batches less than 120 in.<sup>3</sup>, a 5-quart-capacity Hobart Mixer was used. Before mixing, a light coating of silicone grease was applied to the inside of the mixing bowl to help reduce adhesion of the concrete to the side of the bowl. The following mixing procedure (ASTM C 305) was used for both microconcrete and gypsum concrete:

1. All the water was placed in the bowl of the mixer.
2. The cement was added to the water.
3. The mixer was operated at slow speed (140 rpm) for 30 seconds.
4. The entire quantity of sand was added slowly over a 30-second period, while mixing proceeded at slow speed.

5. The mixer was stopped and changed to medium speed (285 rpm), and mixing continued for 30 seconds.

6. The mixer was stopped for 1-1/2 minutes. During the first 15 seconds of this interval, any concrete that may have collected on the side of the bowl was quickly scraped down into the batch. Then, for the remainder of the interval, the bowl was covered with a sheet of plastic film.

7. The mixer was operated for 1 minute at medium speed (285 rpm).

### Casting

The model concretes were consolidated in the forms by a combination of internal and external vibration. A Syntron Vibration Table operated at a frequency of about 38 cps and an amplitude of about 0.05 inch provided the external vibration. For internal vibration, an electric marker equipped with a 2-inch-long shaft (Figure 6) was used.

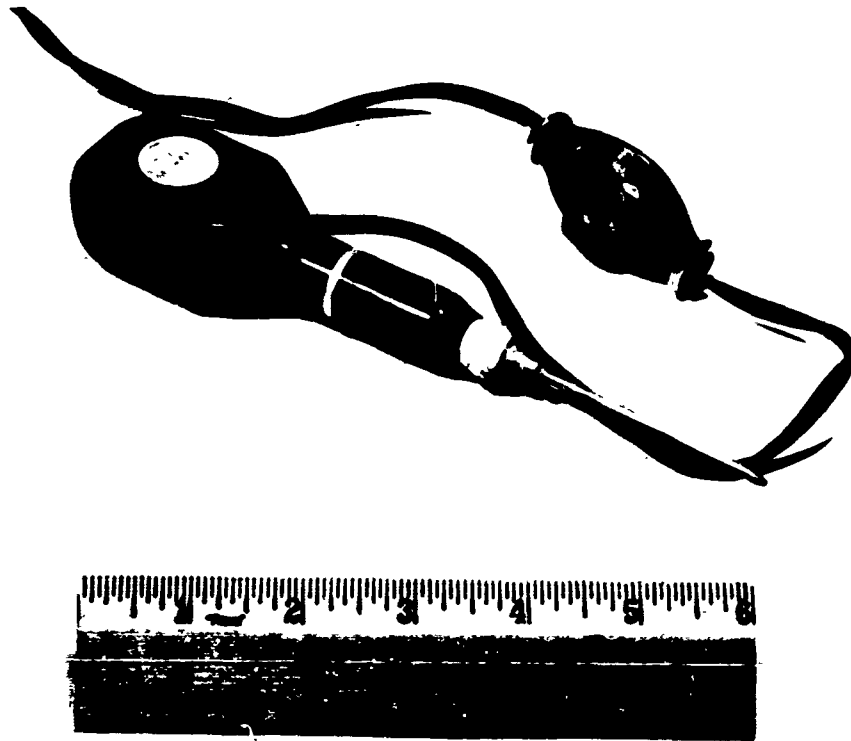


Figure 6. Electric marker equipped with shaft for use as an internal vibrator.

The following procedure was adopted for placing and consolidating both microconcrete and gypsum concrete:

1. The form was fastened or held on the vibration table and the vibrator was turned on.
2. The concrete was placed in the form in two or three layers either by hand or by use of a scoop. For the larger specimens, the concrete was discharged from the hand or scoop evenly over the surface of the specimen.
3. The vibration was continued only long enough to achieve proper consolidation; overvibration caused segregation of the aggregate from the mix. A good indication that sufficient vibration had occurred was when the surface of the concrete became relatively level and many of the air bubbles disappeared from the sides of the form.
4. The remaining air bubbles were removed by moving the shaft of the internal vibrator through the specimen with a slow circular motion while withdrawing it from the specimen. Care was taken not to remove the shaft too quickly as this left a large air void.
5. The excess concrete was screeded off with a straight edge and the surface was finished with a steel trowel.

When casting gypsum concrete, the setting time was often only 15 to 20 minutes. This did not allow a great deal of time to complete the above-mentioned procedure when a large number of forms were to be filled. To provide more time, a retarder can be added to the mixing water to reduce the rate of setting or Ultracal 60 can be used as the cement. A retarder manufactured by the U. S. Gypsum Company has been found satisfactory; a weight ratio of retarder to Ultracal 30 of 0.001 lengthens the time-to-set but does not affect the strength of the concrete.<sup>3</sup>

### **Curing**

**Microconcrete.** After the microconcrete specimens were cast, they were placed in a room maintained at 100% RH and between 70° and 72°F. Twenty-four hours later the specimens were removed from the room for a short time to strip the forms, and were then returned to the room. While the forms were being stripped, damp cloths were wrapped around each specimen to prevent loss of moisture. Curing continued in the 100% RH environment until 2 days before testing, when the specimens were removed and prepared for testing in uncontrolled laboratory conditions, which averaged about 70°F and 50% RH. The effect of the number of days storage at laboratory conditions on compressive strength was investigated and is discussed later.

Each specimen was tested at an age (in days) equal to 12 plus 4 times the specimen diameter or thickness (in inches). This relation between specimen size and age at testing was established by the results of an investigation of the development of compressive strength with age. These results are discussed later.

**Gypsum Concrete.** The forms were removed about 1 hour after the specimens were cast. At an age of 2 hours, the specimens were sealed with two or three coats of shellac to prevent the loss of moisture. The specimens were then stored in the same laboratory conditions as mentioned above and were tested at an age of 2 days.

### **Capping**

The ends of cylinders to be tested in compression were capped with Mineralead\* to provide a plane bearing surface. The aluminum jigs used to cap 1/4 x 1/2-inch and 1 x 2-inch cylinders are shown in Figure 7. Interchangeable bottom plates were used to adapt the larger jig for capping 1-1/2 x 3-inch and 3/4 x 1-1/2-inch cylinders. Microconcrete cylinders were capped during the 2-day period of laboratory storage mentioned above, and gypsum concrete cylinders were capped in the 1-hour period after the forms were removed and before the coating of shellac was applied. For hollow cylinders of gypsum concrete, the inside wall was coated with shellac before capping. Immediately before testing, all shellac was removed from the caps on the gypsum concrete cylinders.

### **Testing**

All specimens were tested in a hydraulically operated universal testing machine with a 120,000-pound capacity. The stressing rate for compression tests was 20 psi/sec (ASTM C 39-64) and for splitting tensile and flexure tests was 100 psi/min. (ASTM C 496-64). In order that all specimens would be tested in the same manner, the loading continued without interruption until failure occurred.

For compression tests the cylinders were placed in a self-aligning Tinius Olsen compression tool with a capacity of 30,000 pounds. Figure 8 shows a typical test setup using this tool. When stress-strain information was desired from a compression test, the strain was measured with two electrical resistance strain gages placed diametrically opposite each other. Gage lengths of 1 inch and 1/2 inch were used on 1-1/2 x 3-inch cylinders

---

\* Atlas Mineral Products Company, Mertztown, Pennsylvania

and 1 (OD) x 5/8 (ID) x 2-inch hollow cylinders, respectively. The gages were wired as two active arms of a wheatstone bridge, and two similar gages constituted the two inactive arms. The sum of the strain in the active gages was read directly from a Baldwin-Lima-Hamilton Type M strain indicator.

The splitting tensile strength of the model concretes was determined by loading two opposite generators of a cylinder (ASTM C 496-64). The load along each generator was applied through a 1/2-inch-square steel bar and two strips of 0.009-inch-thick cardboard. The influence of the number of cardboard strips on the indicated splitting tensile strength was investigated and is discussed later in the report. The operation of aligning the cylinder, steel bars, and cardboard strips in the testing machine was facilitated by the semi-circularly grooved steel blocks shown in Figure 9. The blocks were removed as soon as a small load was applied to the specimen.

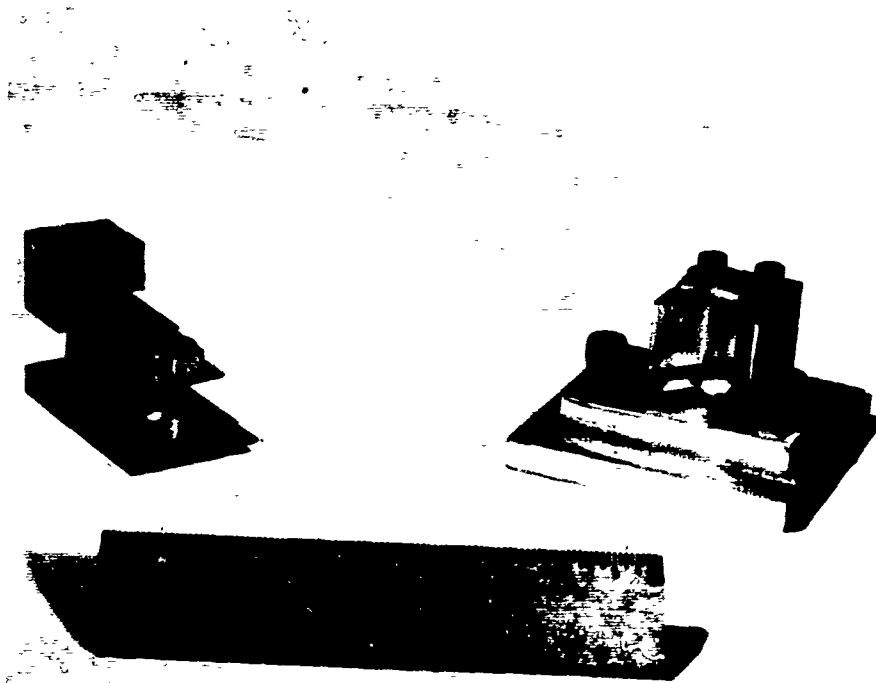


Figure 7. Capping jigs for small cylinders.

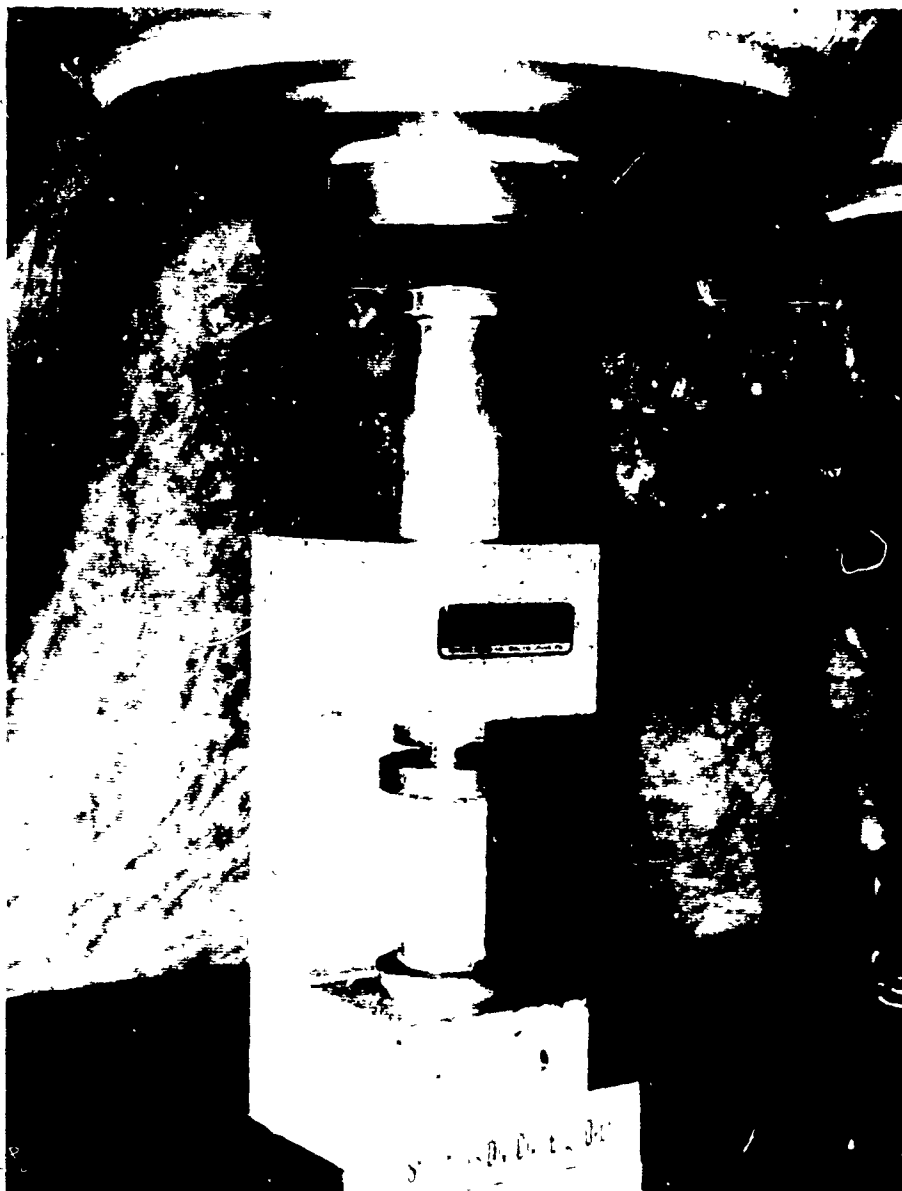


Figure 8. Setup for compression test on 1-1/2 x 3-inch cylinder.

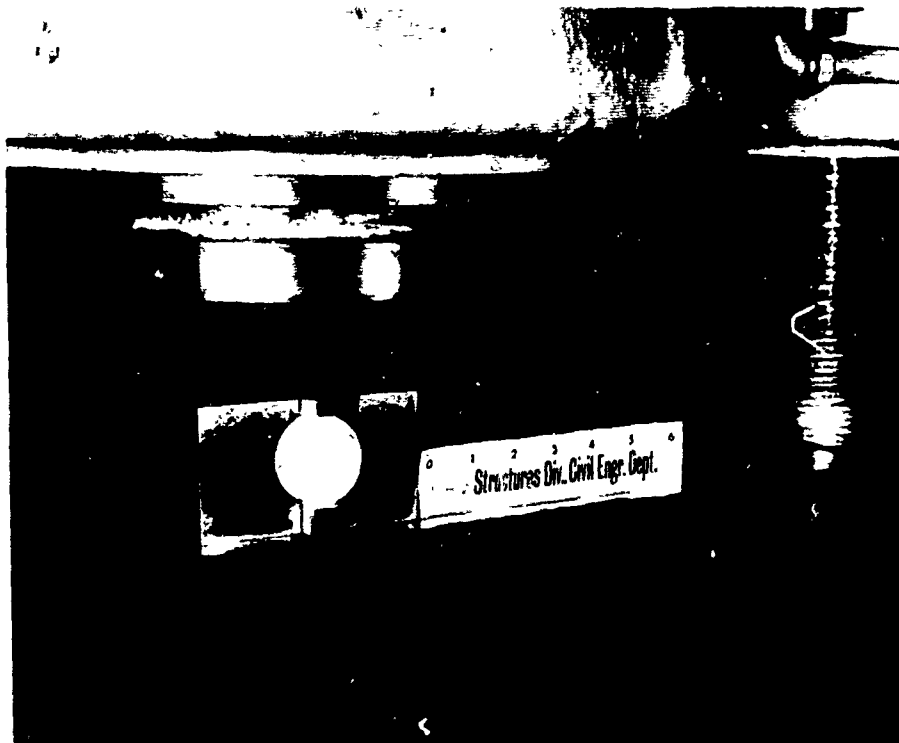


Figure 9. Splitting tensile strength test specimen before load application.

The flexural strength of the model concretes was determined by testing simple beams under third-point loading (ASTM C 78-64). Figure 10 shows the setup for the test of a 1-1/2 x 1-1/2 x 4-1/2-inch (width x depth x span) beam. The third-point loading tool shown in Figure 10 also was used, with suitably adjusted span length and distance between loads, in the testing of 1-1/2 x 3 x 9-inch solid beams and 3 x 3 x 9-inch, 1/4-inch-thick hollow beams.

The hollow beams consisted of two identical channel-shaped halves (Figure 5) that were glued together to form a hollow-box cross section. During testing the beams were oriented with the glue line at the neutral axis. Of the two types of adhesive tried for joining the beam halves, Epocast 8288 was found to be better for this application because of a heavier consistency needed for filling gaps between the surfaces, and a pot life of 45 to 65 minutes.



Figure 10. Setup for flexural strength tests.

The procedure used for gluing the beams was as follows:

1. The surfaces to be glued were thoroughly cleaned with acetone. Care was taken to remove all traces of shellac from the gypsum concrete beams.
2. One hundred parts of Epocast 8288A (epoxy resin) were mixed with 19 parts of Epocast 8288B (hardener), and the mixture was stirred for 5 minutes.
3. A 1/16-inch-thick coat of glue was applied to one-half of the beam with a putty knife, and both halves were pressed together for 30 seconds. The glue was allowed to dry for at least 16 hours before testing.

## RESULTS AND DISCUSSION

### Workability

**Microconcrete.** The flow test (ASTM C 109) was used as the measure of workability. Several combinations of aggregate-cement ratio and aggregate size were used to determine the flow corresponding to the desired condition of workability. For each combination, mixes were prepared having several different flows by varying the water-cement ratio. The mixes which were obviously not too harsh or too wet were cast into appropriately sized cylinders and heavily reinforced beams. In this manner, it was found that mixes having a flow between 103 and 108 cast easily but did not show aggregate segregation during moderate vibration.

After thus defining a quantitative measure of workability, the combinations of aggregate-cement ratio ( $A/C$  ratio  $\geq 1.0$ ) and water-cement ratio which would produce flows within the desired range were determined for six maximum aggregate sizes. The results are shown in Figure 11. In using these results in the design of mixes, care must be taken in scaling values from the curves; for a given water-cement ratio, a change in the aggregate-cement ratio of as little as 0.2 can produce a mix with decidedly different workability characteristics.

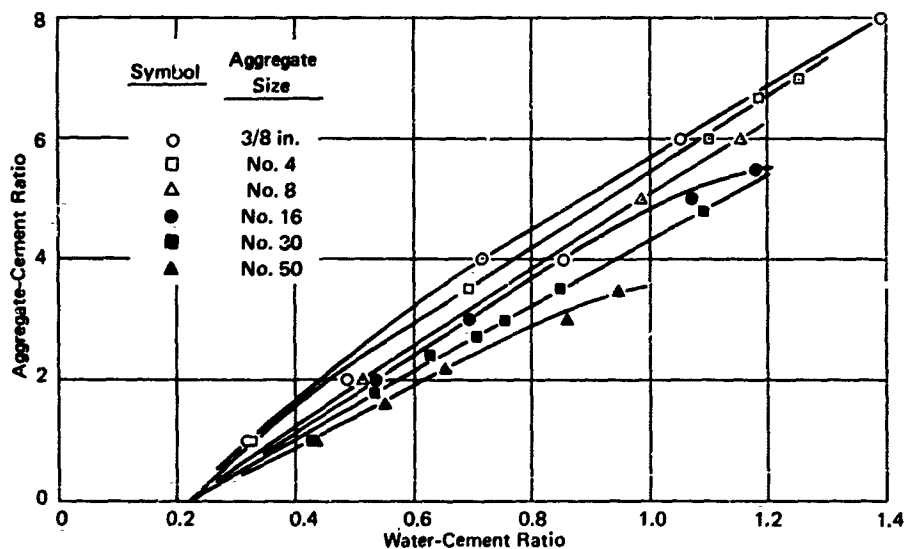


Figure 11. Aggregate-cement ratio versus water-cement ratio for workable mixes of microconcrete and gypsum concrete.

The results shown in Figure 11 for 3/8-inch, No. 4, and No. 8 aggregate plot considerably to the right (that is, greater water-cement ratio for a given aggregate-cement ratio) of the corresponding results reported by Johnson.<sup>5</sup> However, the results for No. 16 aggregate are substantially the same as those obtained by Johnson. This is believed to be due to the different aggregate gradations used in the two investigations. The gradation for No. 16 was nearly the same in this and in Johnson's investigation; the gradations for No. 4 and No. 8 were markedly different. Although factors such as the criterion of workability and the shape of the aggregate particles were probably not the same in the two investigations, the comparison of results serves to point out the strong influence of the aggregate gradation on workability. Therefore, the results shown in Figure 11 can be used in the design of model concrete mixes only when the aggregate gradation for the proposed mix is made the same as the gradation from which the results were derived.

The curves shown in Figure 11 were used to proportion all the microconcrete mixes that will be discussed here.

**Gypsum Concrete.** Gypsum concrete mixes having the previously mentioned quantitative measure of workability (flow between 103 and 108) often began to set before completion of the flow test. Mixes made to the proportions shown in Figure 11 had too large a flow to measure. However, these mixes could be consolidated easily and did not show aggregate segregation during moderate vibration. Therefore, it was decided to use the workability curves in Figure 11 for gypsum concrete as well as for microconcrete.

As aggregate-cement ratios of less than 1.0 were likely to be useful with gypsum concrete, the results of the investigation of the workability of microconcrete were extrapolated to a water-cement ratio of 0.225 at an aggregate-cement ratio of 0. This water-cement ratio was used in previous work<sup>3</sup> on gypsum concretes having no aggregate. The curves that resulted from the extrapolation (Figure 11) were used in proportioning a number of mixes used in studies described subsequently. The workability of these mixes was always satisfactory.

### **Compressive Strength Versus Age**

**Microconcrete.** After completing the workability curves, the next step in developing the mix design procedure was to define the ages when compressive strength ( $f'_c$ ) tests should be conducted on microconcrete cylinders of various sizes. It was desired to strike a compromise between testing at an early age, which would expedite this and future research programs in modeling, and testing at a later age when the compressive strength is relatively stable and a few days' variation in the age at testing a model does not significantly affect the strength.

To define the ages for testing, microconcretes having aggregate sizes of Nos. 4, 8, and 30 were cast in appropriately sized cylinders and tested at various ages to determine the development of compressive strength with age. The results from each test cylinder are shown in Figure 12. Also shown in Figure 12 are the recommended ages for testing, which were derived from the results of the investigation of strength versus age.

The recommended ages for testing were chosen by saying that a rate of gain in strength of 100 psi per day or less would be taken as an indication of relatively stable compressive strength. When this criterion was applied to smoothed curves placed through the strength-versus-age data (Figure 12), the age for testing became 13, 15, and 18 days for Nos. 30, 8, and 4 aggregate, respectively. These results can be expressed by the equation

$$\text{Age} = 12 + 4d \quad (1)$$

where the age for testing is expressed in days and  $d$  is the cylinder diameter (or wall thickness of a hollow cylinder) in inches. Equation 1 has the advantage of predicting whole-number ages for 1/4-inch increments of cylinder diameter. Unless stated otherwise, strength data on microconcrete presented later in the report were collected at the age given by Equation 1.

**Gypsum Concrete.** As noted previously, the chief advantage of gypsum concrete over microconcrete is the rapid rate of development of compressive strength. As indicated by the test results shown in Figure 13, unsealed cylinders reach a plateau of compressive strength within 3 hours after casting. After about 1 day, the strength of the cylinders again begins to increase, due to loss of moisture to the surrounding environment.

To prolong the period of stable compressive strength, thereby providing time for instrumentation, setup, and testing of a model, a technique of sealing gypsum concrete specimens with shellac has been developed.<sup>3</sup> The results for compression tests on sealed specimens are also shown in Figure 13. Here, it can be seen that the strength remained constant for at least 2 days, then decreased slightly between the second and eighth day.

The strength data presented later in the report were derived from specimens sealed at 2 hours and tested at 2 days. Considering the results shown in Figure 13, it is likely that the data presented subsequently describe quite well the properties of specimens sealed between the ages of 2 and 24 hours and tested at ages of up to 8 days.

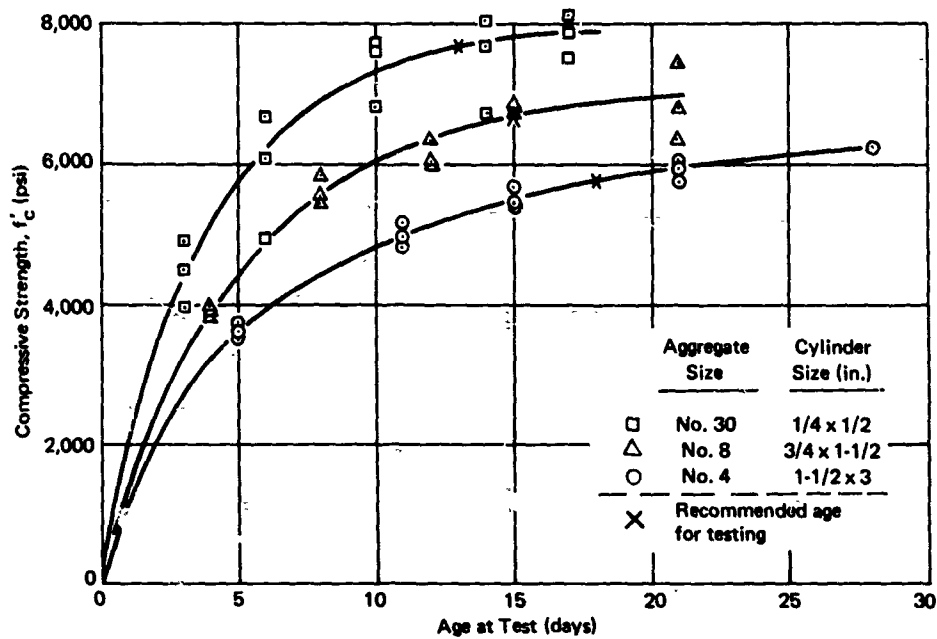


Figure 12. Compressive strength versus age for microconcrete (water-cement ratio = 0.7).

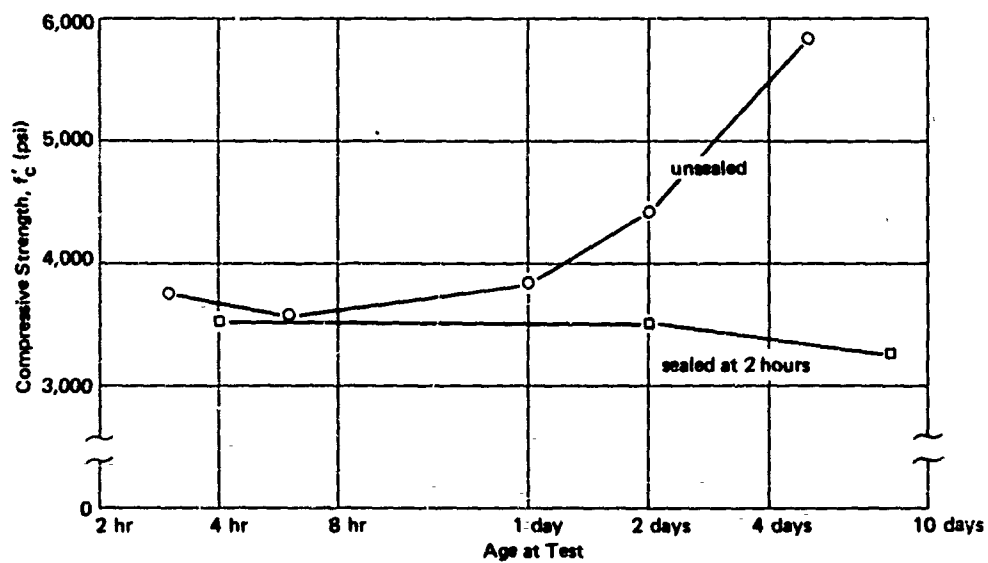


Figure 13. Compressive strength versus age for 1-1/2 x 3-inch cylinder made from gypsum concrete containing No. 4 aggregate (water-cement ratio = 0.325).

## Compressive Strength Versus Water-Cement Ratio

**Microconcrete.** To complete the development of the mix design procedure, tests were conducted to study the relationship between compressive strength and water-cement ratio for microconcretes containing No. 4 and No. 30 aggregates. The average of the results from tests on three cylinders at a number of water-cement ratios is shown in Table 4. Results from tests on individual cylinders are shown in Figures 14 and 15.

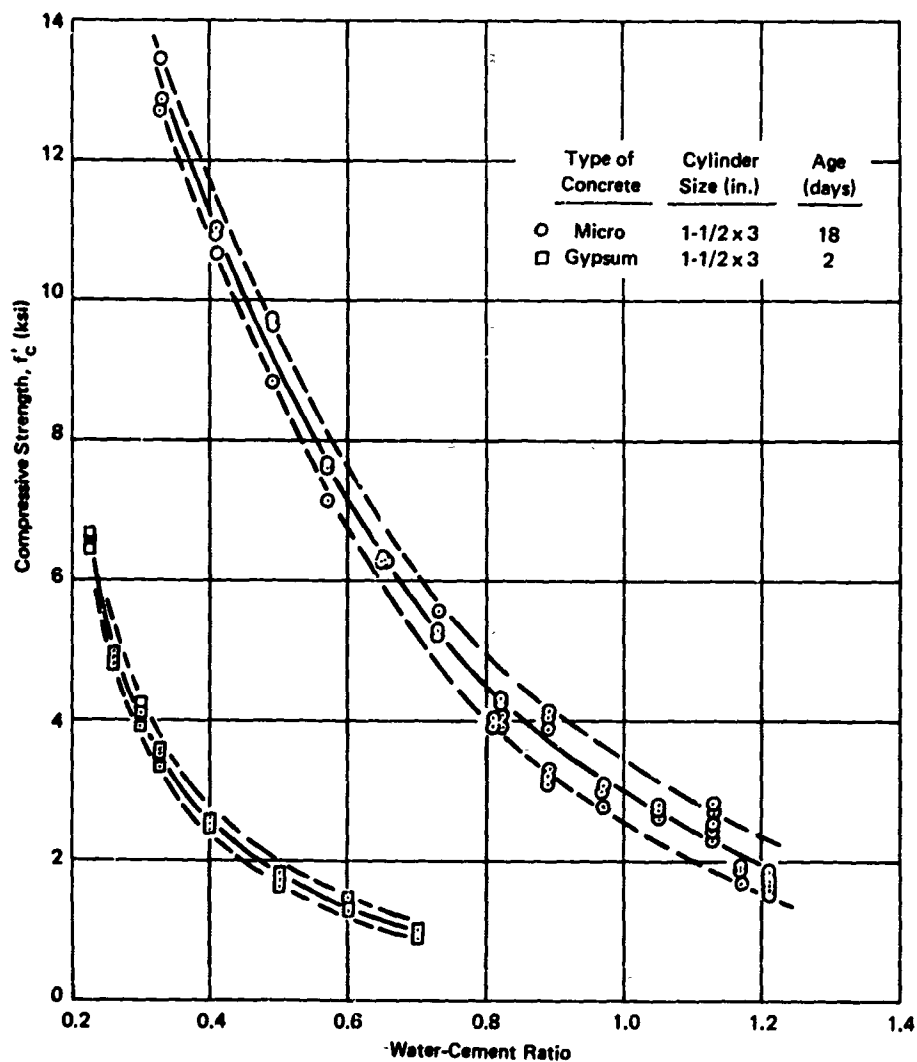


Figure 14. Compressive strength versus water-cement ratio for model concretes containing No. 4 aggregate.

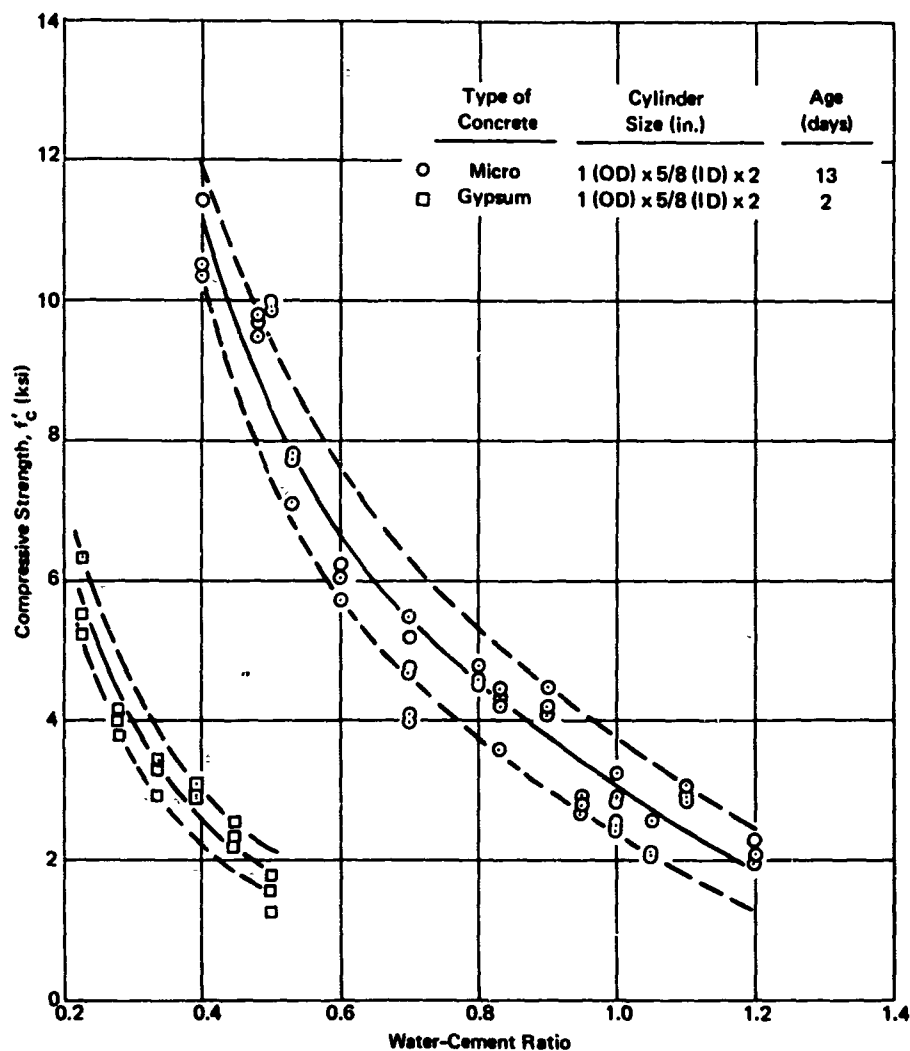


Figure 15. Compressive strength versus water-cement ratio for model concretes containing No. 30 aggregate.

For No. 4 aggregate, average compressive strengths ranging from 13,010 to 1,660 psi were produced by increasing the water-cement ratio from 0.33 to 1.21; the aggregate-cement ratio was selected from workability curves — see Figure 11. In Figure 14, 92% of the test data for the two test cylinders are within  $\pm 400$  psi of the solid-line curve placed through the data. The average strength of all the batches (Table 4) falls within the  $\pm 400$ -psi limits.

Table 4. Average Results From Compressive, Flexural, and Splitting Tensile Tests on Microconcrete 1/

Water-Cement Ratio (by weight)	Aggregate-Cement Ratio (by weight)	Compressive Strength, $f'_c$ $\frac{2}{c}$ (psi)	Splitting Tensile Strength, $f'_{sp}$ $\frac{3}{c}$ (psi)	Flexural Strength, $f'_f$ (psi)		Initial Tangent Modulus of Elasticity, $E_c$ (psi x 10 <sup>6</sup> )	Strain at Maximum Compressive Stress, $\epsilon_o$ (in./in.)
				Small $\frac{4}{c}$ Beam	Large $\frac{5}{c}$ Beam		
No. 4 Aggregate							
0.33	1.04	13,010	498	706	540	—	—
0.41	1.68	10,880	—	—	—	3.99	4,720
0.49	2.25	9,400	674	—	—	—	—
0.57	2.76	7,480	—	—	—	3.43	4,050
0.65	3.28	6,330	580	965	809	—	—
0.73	3.78	5,370	—	—	—	3.45	3,690
0.81	4.28	3,980	366	—	—	—	—
0.82	4.33	4,130 $\frac{5}{c}$	—	—	—	—	—
0.89	4.80	4,020	—	—	—	3.30	—
0.89	4.80	3,210	382	565	455	2.47	3,480
0.97	5.30	2,940	343	—	—	—	—
1.05	5.80	2,770	—	—	—	2.38	2,780
1.13	6.30	2,770 $\frac{1}{c}$	364 $\frac{1}{c}$	435	387	—	—
1.13	6.30	2,440	328	405	398	—	—
1.17	6.55	1,810	—	—	—	—	—
1.21	6.80	1,580	—	—	—	—	—
1.21	6.80	1,740	—	—	—	2.03	2,750
No. 30 Aggregate							
0.40	1.00	10,770	—	—	—	—	—
0.48	1.45	9,670	—	—	—	—	—
0.50	1.60	9,910	—	—	—	—	—
0.53	1.76	7,560	774	—	—	—	—
0.60	2.15	6,010	—	—	—	2.72	4,450

Continued

Table 4. Average Results From Compressive, Flexural, and Splitting Tensile Tests on Microconcrete <sup>1/</sup>

Water-Cement Ratio (by weight)	Aggregate-Cement Ratio (by weight)	Compressive Strength, $f'_c$ <sup>2/</sup> (psi)	Splitting Tensile Strength, $f'_s$ <sup>3/</sup> (psi)	Flexural Strength, $f'_f$ (psi)		Initial Tangent Modulus of Elasticity, $E_c$ (psi x 10 <sup>6</sup> )	Strain at Maximum Compressive Stress, $\epsilon_o$ ( $\mu$ in./in.)
				Small <sup>4/</sup> Beam	Large <sup>5/</sup> Beam		
0.70	2.68	4,270	—	—	—	2.46	3,310
0.70	2.68	5,160	588	—	707	2.75	3,830
0.80	3.23	4,660	—	—	—	—	—
0.83	3.40	4,140 <sup>6/</sup>	—	—	—	—	—
0.90	3.80	4,290	—	—	—	—	—
0.95	4.05	2,820	—	—	—	—	—
1.00	4.32	2,930	—	—	—	2.05	2,990
1.00	4.32	2,670	318	—	—	2.04	2,830
1.05	4.60	2,250	—	—	—	—	—
1.10	4.85	2,960	—	—	—	2.00	4,200
1.20	5.40	2,160	258	—	—	—	—

<sup>1/</sup> Average results from three specimens except where noted otherwise.

<sup>2/</sup> 1-1/2 x 3-in. cylinders for No. 4 aggregate; 1 (OD) x 5/8 (ID) x 2-in. cylinders for No. 30 aggregate.

<sup>3/</sup> 1-1/2 x 3-in. cylinders for No. 4 aggregate; 1 x 2-in. cylinders for No. 30 aggregate.

<sup>4/</sup> Width = 1-1/2 in., depth = 1-1/2 in., span = 4-1/2 in.

<sup>5/</sup> Width = 1-1/2 in., depth = 3 in., span = 9 in.

<sup>6/</sup> Average of 4 cylinders.

<sup>7/</sup> Average of 2 cylinders.

For No. 30 aggregate, compressive strengths ranging from 10,770 to 2,160 psi were produced by increasing the water-cement ratio from 0.4 to 1.2. In Figure 15, 90% of the test data for individual cylinders are within  $\pm 800$  psi of the solid-line curve placed through the test data. The average strength of two of the batches falls outside the  $\pm 800$ -psi limits.

When the test results for the No. 4 and the No. 30 aggregates (Figures 14 and 15) are compared, the smaller scatter of the data for the No. 4 aggregate is immediately evident. Not so evident is the fact that the mean (solid line) curves through the data for the two sizes of aggregate are essentially identical for water-cement ratios between 0.75 and 1.20. The maximum difference between the mean curves is about 650 psi at a water-cement ratio of 0.50.

The data for No. 30 aggregate were obtained from tests on hollow cylinders having an outside diameter, inside diameter, and height of 1, 5/8, and 2 inches, respectively. The hollow cylinders were used because in earlier tests (Figure 12) large differences in strength were obtained from three supposedly identical 1/4 x 1/2-inch cylinders. Also, it was much easier to cast, cap, and test the hollow cylinders than the smaller solid cylinders. The correlation between results from tests of hollow cylinders and those from tests of 1/4 x 1/2-inch solid cylinders is discussed later. Some hollow cylinders after testing are shown in Figure 16.



Figure 16. Hollow cylinders after compressive strength tests.

As mentioned previously, all microconcrete specimens were dried in the laboratory environment for 2 days before testing. This was done to simulate the time necessary to prepare for and conduct a model test. In some cases, shorter periods of drying might be used to reduce the probability of developing significant shrinkage strains in a model. When the shorter drying time is anticipated, the data shown in Figure 17 can be used in mix design to correct the compressive strength test results shown in Figures 14 and 15.

**Gypsum Concrete.** Average results of compressive strength tests on gypsum concretes having No. 4 and No. 30 aggregate and various water-cement ratios are listed in Table 5. Results for individual cylinders are shown in Figures 14 and 15.

For No. 4 aggregate, compressive strengths ranging from 6,590 to 960 psi were produced by increasing the water-cement ratio from 0.225 to 0.70; the aggregate-cement ratio was selected from workability curves — see Figure 11. In Figure 14, all the data for individual cylinders are within  $\pm 200$  psi of the solid-line curve placed through the test data.

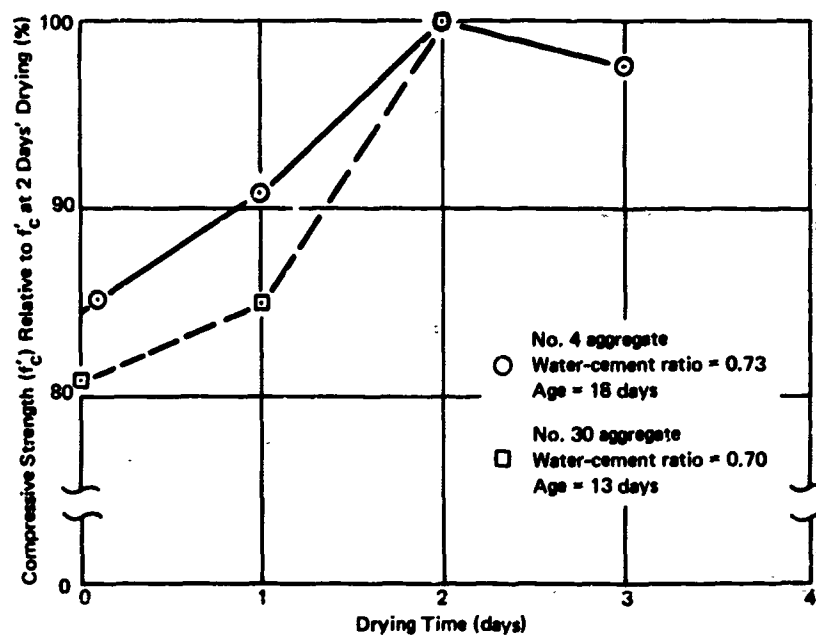


Figure 17. Effect of length of drying time on compressive strength of microconcrete.

Table 5. Average Results From Compressive, Flexural, and Splitting Tensile Tests on Gypsum Concrete <sup>1/</sup>

Water-Cement Ratio (by weight)	Aggregate-Cement Ratio (by weight)	Compressive Strength, $f'_c$ <sup>2/</sup> (psi)	Splitting Tensile Strength, $f'_{sp}$ <sup>3/</sup> (psi)	Flexural Strength, $f'_f$ (psi)		Initial Tangent Modulus of Elasticity, $E_c$ (psi x 10 <sup>6</sup> )	Strain at Maximum Compressive Stress, $\epsilon_o$ ( $\mu$ in./in.)
				Small <sup>4/</sup> Beam	Large <sup>5/</sup> Beam		
No. 4 Aggregate							
0.225	0	6,590	—	—	—	3.01	3,160
0.260	0.35	4,900	441	789	718	—	—
0.300	0.76	4,080	—	—	—	2.80	—
0.325	1.00	3,510	257	—	—	2.45	2,600
0.400	1.60	2,530	200	416	403	—	—
0.500	2.30	1,730	—	—	—	2.15	1,480
0.600	2.95	1,380	—	—	—	—	—
0.700	3.58	960	—	—	—	—	—
No. 30 Aggregate							
0.225	0	5,700	—	—	—	—	—
0.280	0.30	3,990	413	—	—	2.31	2,120
0.335	0.60	3,210	—	—	—	—	—
0.390	0.92	2,980	—	—	—	2.67	1,780
0.445	1.26	2,370	—	—	—	—	—
0.500	1.60	1,530	—	—	—	2.14	970

<sup>1/</sup> Average results from three specimens except where noted otherwise.

<sup>2/</sup> 1-1/2 x 3-in. cylinders for No. 4 aggregate; 1 (OD) x 5/8 (ID) x 2-in. cylinders for No. 30 aggregate.

<sup>3/</sup> 1-1/2 x 3-in. cylinders for No. 4 aggregate; 1 x 2-in. cylinders for No. 30 aggregate.

<sup>4/</sup> Width = 1-1/2 in., depth = 1-1/2 in., span = 4-1/2 in.

<sup>5/</sup> Width = 1-1/2 in., depth = 3 in., span = 9 in.

For No. 30 aggregate, compressive strengths ranging from 5,700 to 1,530 psi were produced by increasing the water-cement ratio from 0.225 to 0.50. In Figure 15, 94% of the data for individual cylinders are within  $\pm 500$  psi of the solid-line curve placed through the test data.

When the results for the No. 4 and the No. 30 aggregates (Figures 14 and 15) are compared, the smaller scatter of the data for the No. 4 aggregate is evident. The mean (solid-line) curves through the data for the two sizes of aggregate are essentially identical for water-cement ratios between 0.30 and 0.50. For water-cement ratios less than 0.30, the strengths of the No. 30 aggregate concretes are less than the strengths of the No. 4 aggregate concretes, with the maximum difference being 700 psi at a water-cement ratio of 0.225. Since the concretes at a water-cement ratio of 0.225 had no aggregate, it is likely that the difference between the mean curves for No. 30 and No. 4 aggregates is more a result of differences in the shape of test specimens used than of the differences in the size and amount of aggregate. Other evidence supports this view; the hollow test cylinders for concrete with a water-cement ratio of 0.225 and 0.28 failed by vertical splitting, rather than by the compressive crushing (Figure 16) noted at other water-cement ratios.

For the same cylinder size, the scatter bands (dotted lines in Figures 14 and 15) on the gypsum concrete results are about half as wide as the bands on the microconcrete results. There are two likely explanations for this: (1) It was easier to properly consolidate gypsum concrete cylinders than microconcrete cylinders (only occasionally were sizable air voids found in failed gypsum concrete specimens); (2) The scatter of the microconcrete results was probably increased by the 2 days of drying in an uncontrolled environment. Although the gypsum concrete cylinders were stored in the same environment, sealing of the specimens made them relatively insensitive to the surrounding conditions.

### Splitting Tensile Strength

**Influence of Number of Bearing Strips.** The standard splitting tensile strength ( $f'_{sp}$ ) test for prototype concrete (ASTM C 496-64) employs plywood bearing strips, 1/8 inch thick by 1 inch wide. Direct modeling of the standard test to 1-1/2 x 3-inch cylinders would require 0.03-inch-thick plywood, a thickness not generally available. In the testing of 3 x 6-inch cylinders, thin cardboard bearing strips have been used, and it was found that varying the width and thickness of the cardboard had no significant effect on the indicated splitting tensile strength.<sup>7</sup>

To determine the influence, if any, of the thickness of the bearing material on the splitting tensile strength of 1-1/2 x 3-inch cylinders, tests were conducted on cylinders from the same batch of microconcrete with 0, 1, 2, and 4 strips of 0.009-inch-thick cardboard being used along each of the loaded generators of the cylinders. The results of the tests are shown in Figure 18 and indicate that the splitting tensile strength was not significantly influenced by the number of strips. For example, the average strengths were 353 psi and 374 psi for zero and four bearing strips, respectively. Although probably a fortuitous happening, the close grouping of the results from the three cylinders tested with two bearing strips was encouraging. Two bearing strips were used in all the splitting tensile tests from which results are reported later.

**Prototype Concrete.** Splitting tensile strength versus compressive strength data for prototype concrete were collected from several sources<sup>8-14</sup> to provide a basis for comparing the splitting tensile strengths of prototype and model concretes. The data are shown in Figure 19.

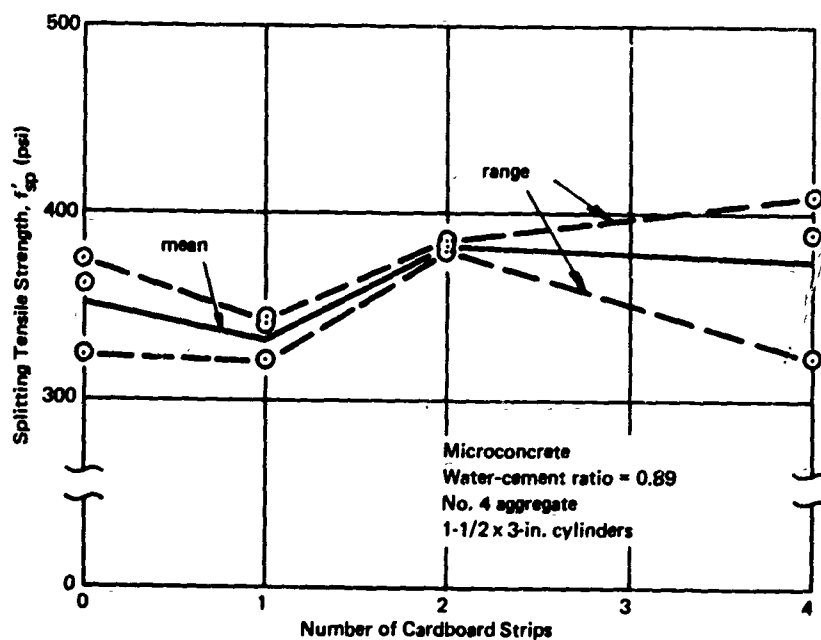


Figure 18. Influence of number of cardboard bearing strips on splitting tensile strength.

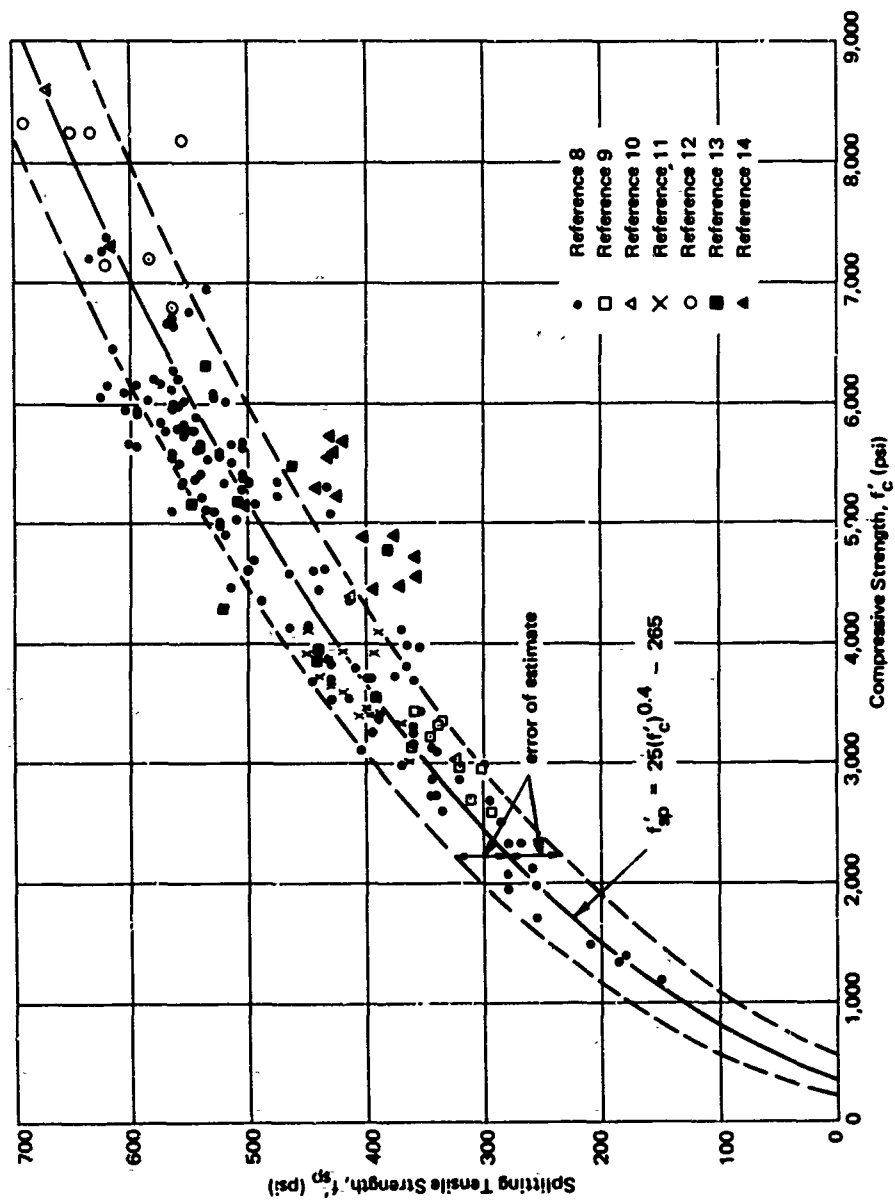


Figure 19. Splitting tensile strength versus compressive strength of prototype concrete.

Linear regression analyses were performed to find the constants  $m$ ,  $a$ , and  $b$  to make the equation

$$f'_{sp} = a(f'_c)^m + b \quad (2)$$

best fit the data shown in Figure 19. A portion of the results from the analyses is presented in Table 6. These results indicate that a large number of values for  $m$ , with appropriate constants  $a$  and  $b$ , can be used in Equation 2 without significantly changing the fit of the equation to the data. However, the best fit (highest correlation coefficient and lowest error of estimate) was obtained from the equation

$$f'_{sp} = 25(f'_c)^{0.4} - 265 \quad (3)$$

Equation 3 is plotted in Figure 19.

Table 6. Results of Regression Analyses of Splitting Tensile Strength Data

$m$ <sup>1/</sup>	$a$ <sup>2/</sup>	$b$ <sup>3/</sup> (psi)	Correlation Coefficient (%)	Error of Estimate (psi)
0.35	43.2	-361	91.07	45.33
0.39	27.8	-282	91.08	45.31
0.40	25.0	-265	91.08	45.30
0.41	22.4	-248	91.08	45.31
0.45	14.7	-189	91.07	45.33
0.50	8.71	-128	91.05	45.39
0.55	5.23	-78	91.01	45.48
0.60	3.16	-36	90.95	45.61
0.65	1.92	-1	90.89	45.76
0.70	1.17	30	90.81	45.94
1.00	0.0662	150	90.12	47.56

<sup>1/</sup>  $m$  = exponent of  $f'_c$  in Equation 2.

<sup>2/</sup>  $a$  = coefficient of  $f'_c$  in Equation 2.

<sup>3/</sup>  $b$  = pure constant in Equation 2.

**Microconcrete.** The results of splitting tensile strength tests on microconcretes containing No. 4 and No. 30 aggregates are given in Table 4 and Figure 20. Figure 20 also shows a plot of Equation 3, with the error of estimate indicated by dotted lines.

With the exception of the data for concrete with a water-cement ratio of 0.33 (Table 4 — not shown in Figure 20), Figure 20 indicates that the relationship between  $f'_{sp}$  and  $f'_c$  is about the same for microconcrete containing No. 4 aggregate as for prototype concrete. For the microconcretes containing No. 30 aggregate, tested in 1 x 2-inch cylinders,  $f'_{sp}$  appears to be about the same as for prototype concrete at low  $f'_c$ , but higher than for prototype concrete at high  $f'_c$ .

The use of 1 x 2-inch cylinders for determining  $f'_{sp}$  of the No. 30 aggregate microconcretes violates the approach discussed earlier for choosing the size of test specimen. The original test plans proposed obtaining a measure of the tensile strength of the No. 30 aggregate concretes by conducting splitting tensile strength tests on 1/4 x 1/2-inch cylinders and flexural tests on 1/4-inch-thick hollow beams. However, conducting splitting tensile strength tests on the small cylinders did not prove practical; the tests were extremely difficult to perform and the results appeared to be meaningless (an  $f'_{sp}$  value exceeding 3,000 psi was obtained). When the results from hollow beams proved to be of questionable value (see later discussion), an expeditious means was sought for gaining an indication of the tensile properties of the No. 30 aggregate concretes. At that time, 1 x 2-inch cylinders were chosen for use. This size of cylinder was easy to test, fractured as desired, and gave extremely consistent results (little scatter in the test data for three identical specimens).

**Gypsum Concrete.** The results of splitting tensile strength tests on gypsum concrete containing No. 4 and No. 30 aggregates respectively, are given in Table 5 and Figure 20. A 1-1/2 x 3-inch cylinder after testing is shown in Figure 21.

On the basis of limited testing, the results in Figure 20 indicate that for comparable  $f'_c$  the gypsum concretes with No. 4 aggregate have a lower  $f'_{sp}$  than prototype concrete. This finding -- lower  $f'_{sp}$  for gypsum concrete than for prototype concrete -- contradicts previous findings,<sup>3</sup> where the  $f'_{sp}$  for gypsum concretes was generally toward the upper edge of the scatter band of  $f'_{sp}$  data for prototype concrete.

The data in Figure 20 for the one splitting tensile strength test conducted on gypsum concrete containing No. 30 aggregate are seen to be nearly the same as the  $f'_{sp}$  data for prototype concrete having the same  $f'_c$ .

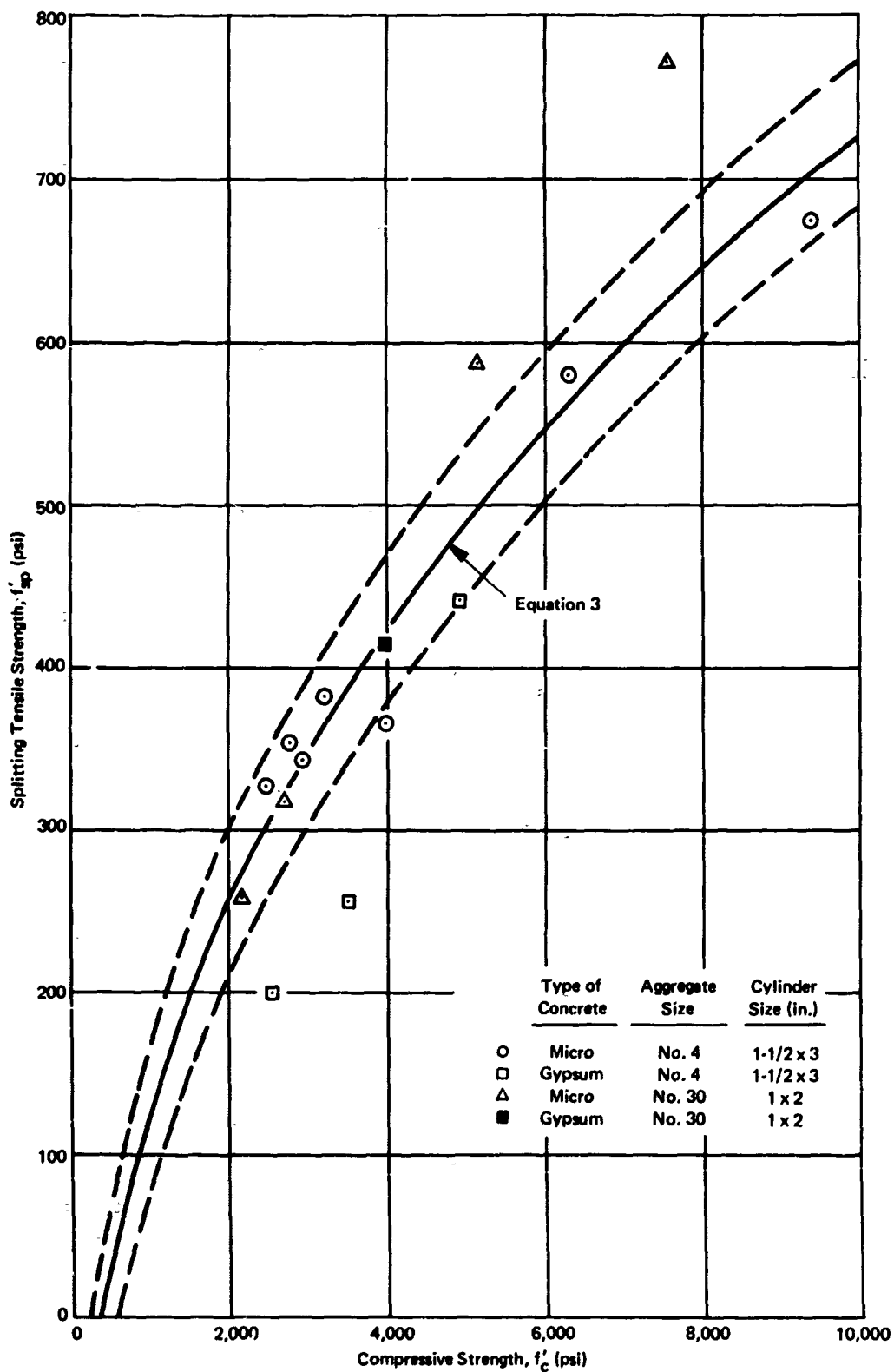


Figure 20. Comparison of splitting tensile strengths of model and prototype concretes.

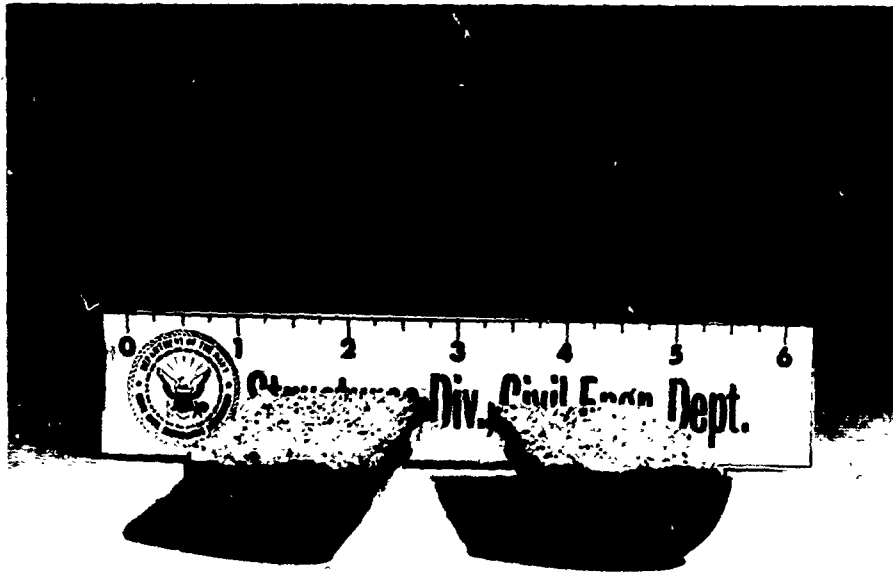


Figure 21. Gypsum concrete cylinder after splitting tensile strength test.

#### Flexural Strength of Concretes

**Prototype Concrete.** The correlations of the results from flexural strength ( $f'_f$ ) and splitting tensile strength tests on prototype concrete, as reported in References 8 and 15, are shown in Figure 22. The average of the correlations for gravel and crushed-stone concretes from Reference 8 is described approximately by the equation

$$f'_f = 1.55 f'_{sp} \quad (4)$$

and the correlation from Reference 15 is described approximately by the equation

$$f'_f = f'_{sp} + 250 \quad (5)$$

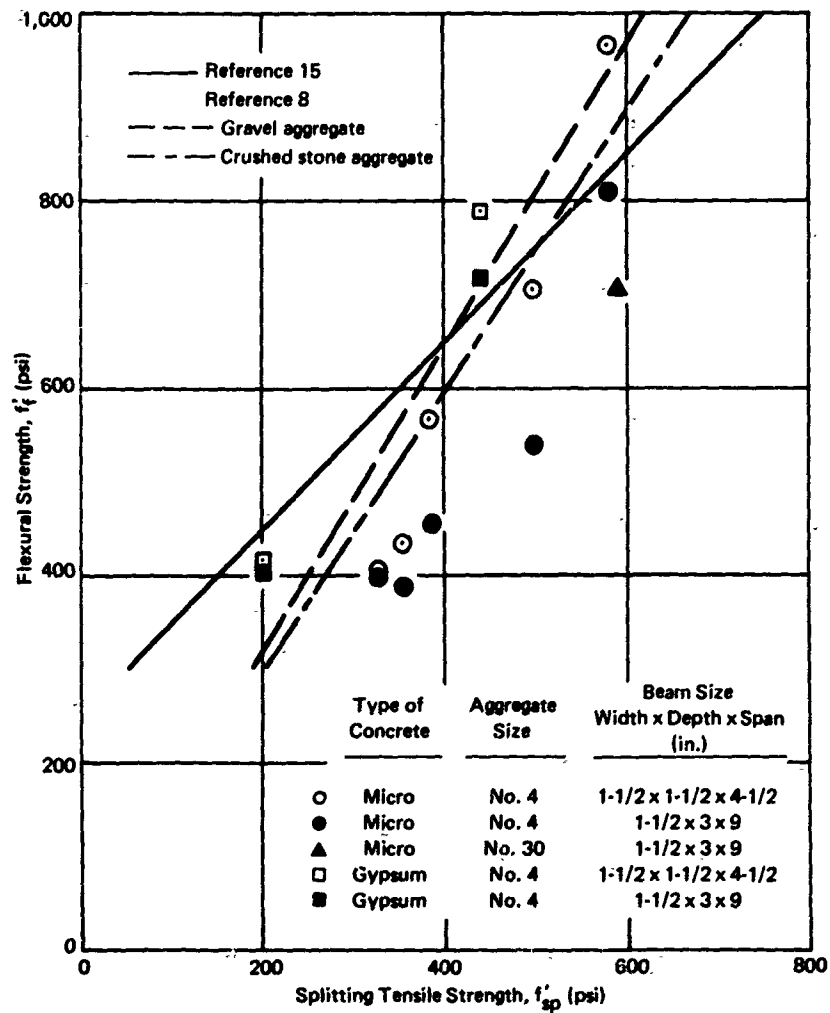


Figure 22. Correlation between flexural strength and splitting tensile strength.

By combining Equations 4 and 3 and Equations 5 and 3, two equations relating  $f'_f$  to  $f'_c$  were obtained:

$$f'_f = 39(f'_c)^{0.4} - 411 \quad (6)$$

$$f'_f = 25(f'_c)^{0.4} - 15 \quad (7)$$

Equations 6 and 7 are plotted in Figure 23.

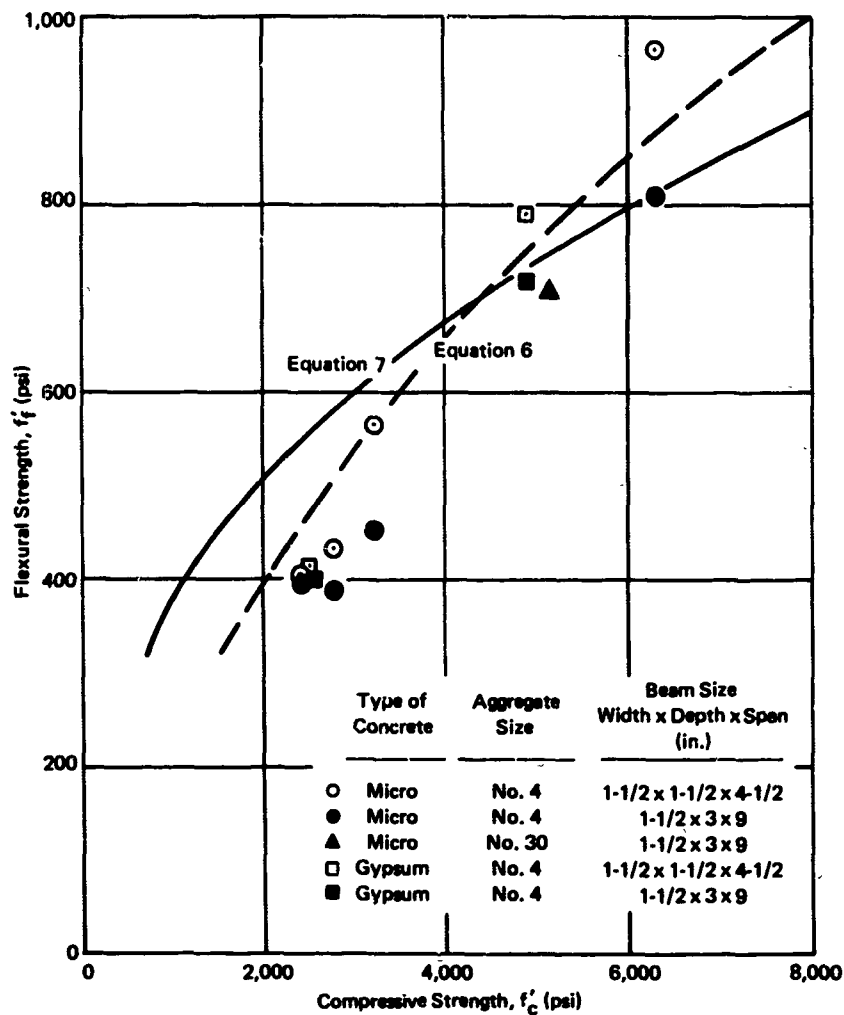


Figure 23. Comparison of flexural strengths of model and prototype concretes.

**Microconcrete.** The results from flexural tests on microconcrete are shown in Table 4 and in Figures 22 and 23. For the No. 4 aggregate concretes tested in the smaller (1-1/2 x 1-1/2 x 4-1/2-inch) beams, which were scaled directly from the standard ASTM beam, Figure 22 shows about the same correlation between  $f'_f$  and  $f'_{sp}$  as reported for gravel concretes in Reference 8. For the larger (1-1/2 x 3 x 9-inch) microconcrete beams,  $f'_f$  was always less than would be expected for a prototype concrete having the same  $f'_{sp}$ .

Figure 23 shows that, except for a water-cement ratio of 0.33 (not plotted in the figure), the flexural strength data for the smaller microconcrete beams correlate reasonably well with the relation between  $f'_t$  and  $f'_c$  given by Equation 6 for prototype concrete. Except for concrete with a compressive strength of 6,300 psi, the flexural strength of the larger microconcrete beams was less than would be expected for a prototype concrete having the same  $f'_c$ ; this agrees with the prediction from Equation 7.

**Gypsum Concrete.** The results from flexural tests on gypsum concrete are listed in Table 5 and shown in Figures 22 and 23. A group of beams after testing is shown in Figure 24. The beams in this figure are typical of both microconcrete and gypsum concrete specimens; without exception, failures occurred in the middle third of the span.

On the basis of a limited number of tests, the results in Figures 22 and 23 indicate that the  $f'_t$  versus  $f'_{sp}$  and  $f'_t$  versus  $f'_c$  relationships are about the same for gypsum concrete as for prototype concrete. For microconcrete, the  $f'_t$  results from testing the smaller beams more closely approximated the results from prototype concrete than did the results from testing the larger beams; for gypsum concrete, no such trend is apparent.

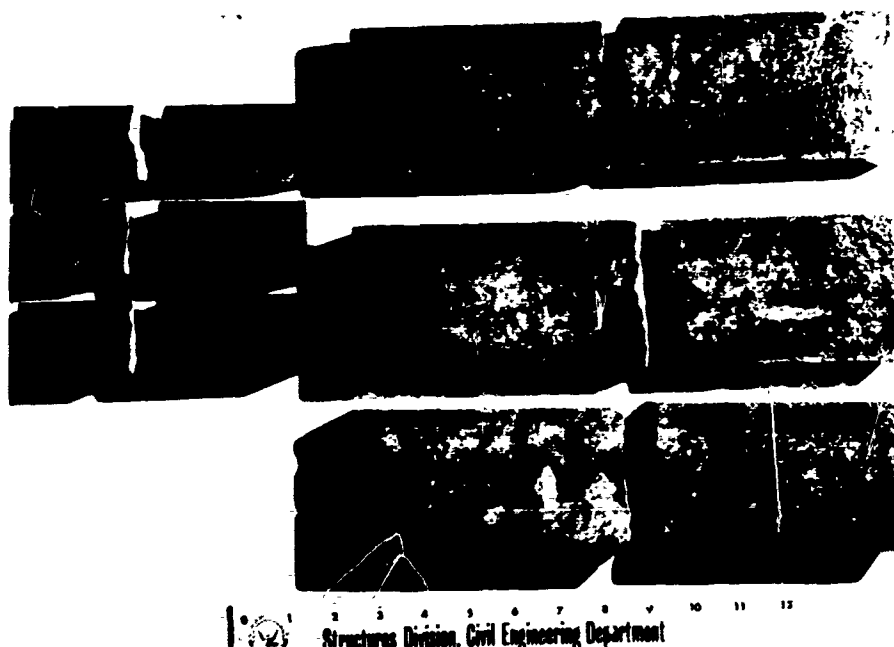


Figure 24. Gypsum concrete beams after testing.

## Flexural Strength of Hollow Beams

Attempts were made to obtain a measure of the tensile strengths of the model concretes containing No. 30 aggregate by conducting flexural tests on 1/4-inch-thick hollow beams. As mentioned previously, two types of adhesive were tried for joining the two halves of the beams. During testing, the beams were oriented with the glue-line at the neutral axis. For the beam halves joined with Epocast 8288 epoxy resin, no glue-line failures were noted on microconcrete beams and only one glue-line failure was noted on gypsum concrete beams. The results of flexural strength tests from beams where no glue-failure was noted are shown in Figure 25. A group of fractured microconcrete beams that were glued with Epocast 8288 epoxy resin is shown in Figure 26. The failure zone of one of the beams is shown in Figure 27. For the beam halves joined with the other adhesive, glue-line failures often occurred before tensile fracture of the beam at the bottom fiber.

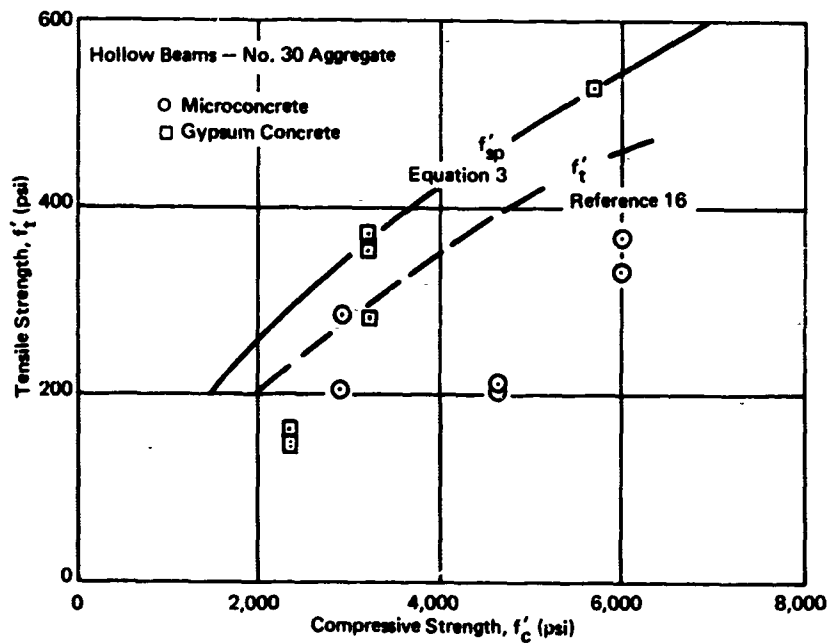


Figure 25. Flexural strength ( $f'_f$ ) of hollow beams compared with tensile strength of prototype concrete measured directly ( $f'_t$ ) and by splitting ( $f'_{sp}$ ).

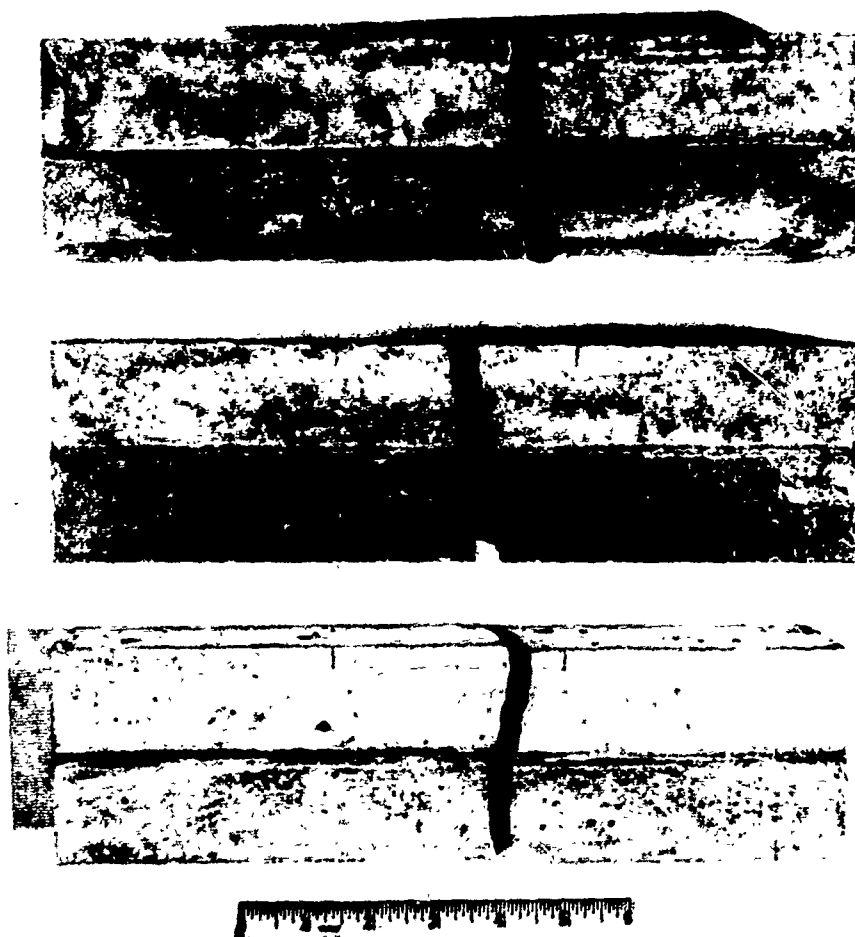


Figure 26. Microconcrete hollow beams after testing.



Figure 27. Failure zone of microconcrete hollow beam.

The tensile strength data plotted in Figure 25 are the computed stresses at the middle of the 1/4-inch-thick lower flange of the hollow beams when the beams failed under flexural strength testing. Because the strain field in the lower flange of the beams was nearly uniform and therefore strain gradient effects should be small, it was thought that the results of flexural strength tests on hollow beams might be as good a measure of the tensile strength as are splitting tensile strength test results. In fact, the  $f_t'$  results from tests on three of the gypsum concrete hollow beams correlated exceedingly well with the  $f_{sp}'$  results for prototype concrete (Figure 25). However, the hollow beam  $f_t'$  results from a gypsum concrete of low  $f_c'$  were much lower than either the expected  $f_{sp}'$  or direct tensile strength,  $f_t'$ . This is a trend similar to that exhibited by gypsum concretes containing No. 4 aggregate (Figures 20 and 23), where the tensile strength appeared to be low relative to the tensile strength of prototype concrete when  $f_c'$  was low.

For the microconcrete hollow beams, the values for  $f_t'$  tests, with one exception, were much lower than the values from  $f_t'$  tests of prototype concrete (Figure 25).<sup>16</sup> This is contrary to the  $f_{sp}'$  test findings discussed earlier (see Figure 20), which indicated that the microconcretes with No. 30 aggregate have about the same tensile strength as prototype concrete. The low values for tensile strength from tests of microconcrete hollow beams may be due to the effects of shrinkage strains induced in the specimens during the 2-day period of drying.

Subject to further experimental confirmation, it appears that flexural strength tests on hollow beams can be used to provide a measure of the tensile strength of thin layers of sealed gypsum concrete. Such tests do not appear to yield useful information on microconcrete cured under the conditions used in this investigation. It is noted that the manufacture of hollow beams of the configuration tested was a difficult, time-consuming process. Stripping a beam half of its form required the removal of more than 30 screws, and a number of beam halves were cracked during this operation.

### Stress-Strain Relation in Compression

**Prototype Concrete.** A number of mathematical expressions have been proposed to describe the stress-strain relation of prototype concrete in compression. One of the most widely used expressions was proposed in Reference 17. For  $\epsilon \leq \epsilon_o$ , this expression is

$$f_c = f_c' \left[ 2 \frac{\epsilon}{\epsilon_o} - \left( \frac{\epsilon}{\epsilon_o} \right)^2 \right] \quad (8)$$

where  $f_c$  is the stress corresponding to a strain  $\epsilon$  and  $\epsilon_o$  is the strain corresponding to the peak stress,  $f'_c$ . Also from Reference 17,

$$E_c = 1,800,000 + 460 f'_c \quad (9)$$

and 
$$\epsilon_o = \frac{2 f'_c}{E_c} \quad (10)$$

where  $E_c$  is the initial tangent modulus of elasticity. Using Equation 8, the secant moduli to stresses of 50 and 90%  $f'_c$  become  $0.854 E_c$  and  $0.658 E_c$ , respectively.

The initial tangent modulus for a particular concrete often differs considerably from the value given by Equation 9. For example, Figure 23 shows the results reported in Reference 18 as well as a plot of Equation 9. Similarly, oftentimes the unique relationship between  $\epsilon_o$  and  $f'_c$  implied by Equations 9 and 10 is not discernible from tests on particular concretes.

**Microconcrete.** Table 4 shows the  $E_c$  and  $\epsilon_o$  determined from compression tests on some of the microconcretes. These test results are compared with corresponding results for prototype concrete in Figures 28 and 29. Data on the secant moduli to 50 and 90%  $f'_c$  are presented in Figures 30 and 31, where the expected moduli for prototype concrete also are shown.

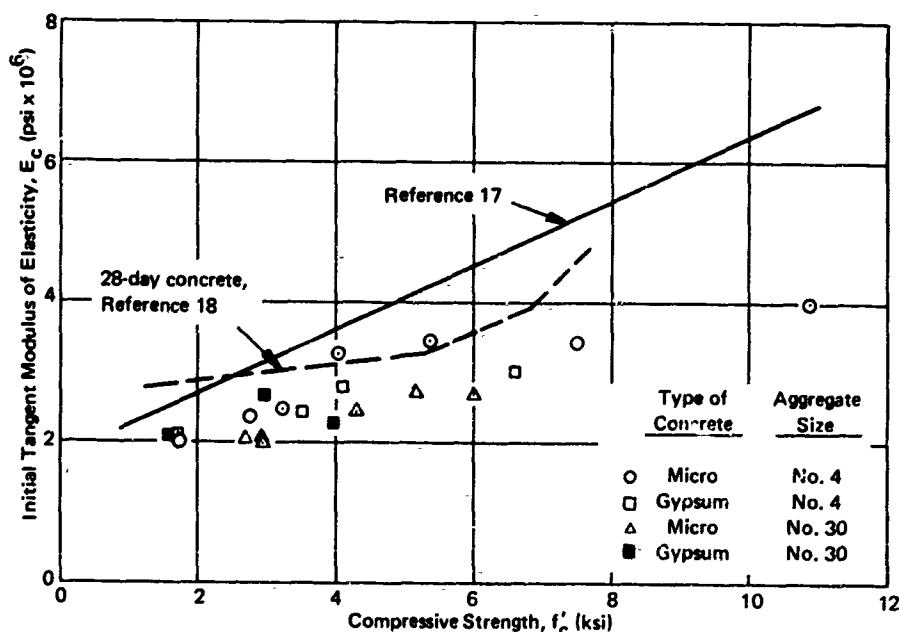


Figure 28. Modulus of elasticity versus compressive strength for model concretes.

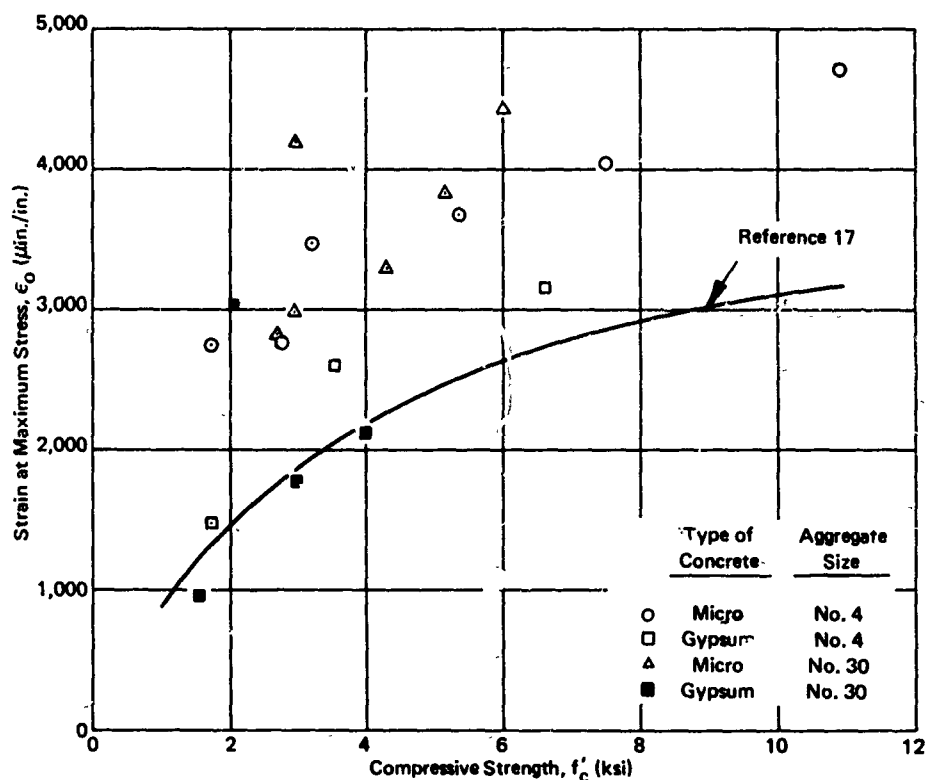


Figure 29. Strain at maximum stress versus compressive strength for model concretes.

From Figure 28 it can be seen that for a particular  $f'_c$ , the  $E_c$  for the microconcretes was less than for prototype concrete. Also, for a given  $f'_c$ , the  $E_c$  was slightly higher for the microconcretes containing No. 4 aggregate than for those containing No. 30 aggregate.

From Figure 29, the  $\epsilon_0$  for the microconcretes was greater than for prototype concrete. On the average, the  $\epsilon_0$  was greater for the microconcrete containing No. 30 aggregate than for that containing No. 4 aggregate, although for some compressive strengths there was little difference.

Information on the shapes of the microconcrete stress-strain curves and the prototype concrete stress-strain curves are compared in Figures 30 and 31. These figures show that the majority of the data points for microconcrete fall below the line for prototype concrete. This indicates that the microconcrete stress-strain curves bend over slightly more rapidly than do the prototype concrete stress-strain curves. In this respect, the No. 4 aggregate microconcretes appear to depart more from the prototype concrete curve than do the No. 30 aggregate microconcretes; however, in either case, the departure is not large.

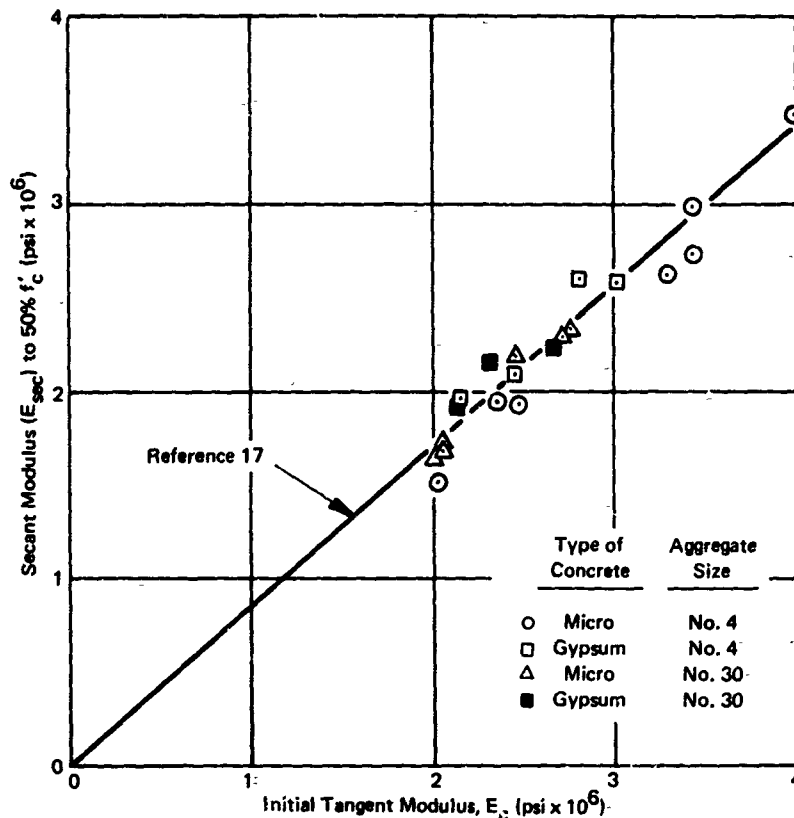


Figure 30. Comparison of secant modulus (to 50%  $f'_c$ ) with initial tangent modulus for four concrete mixes.

**Gypsum Concrete.** Table 5 and Figures 28 through 31 show data on the stress-strain relation for gypsum concrete in compression.

For a particular  $f'_c$  (Figure 28), the  $E_c$  for the gypsum concretes is less than for prototype concrete. There appears to be very little difference between gypsum concrete and microconcrete in the  $E_c$  for a given  $f'_c$ .

From Figure 29, the gypsum concretes simulate  $\epsilon_o$  for prototype concrete much better than do the microconcretes. In fact, the results for gypsum concrete containing No. 30 aggregate are nearly identical to the predictions of Equation 10. Combining this observation with the previous observation that the microconcretes have a lower  $E_c$  than prototype concrete has, it can be concluded that the stress-strain curve for the No. 30 aggregate gypsum concrete is more nearly linear than the stress-strain curve for prototype concrete. This conclusion is reinforced by the results in Figures 30 and 31, which show the curves of the secant moduli to be above the curves of secant moduli for prototype concrete.

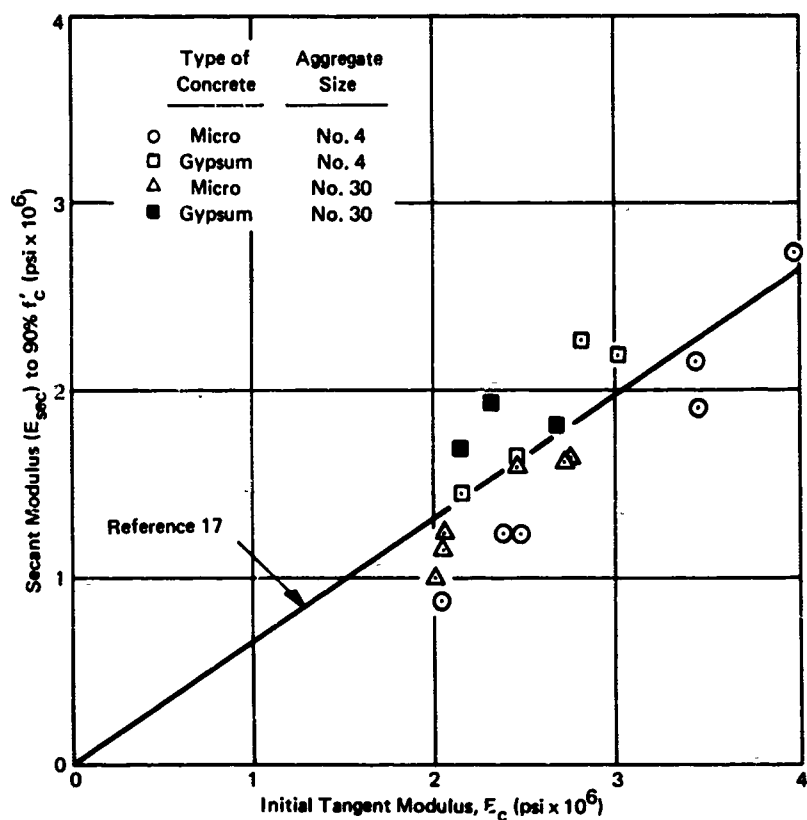


Figure 31. Comparison of secant modulus (to 90%  $f'_c$ ) with initial tangent modulus for four concrete mixes.

Figures 30 and 31 show the shape of the stress-strain curves for gypsum concretes containing No. 4 aggregate to be very similar to the shape of the curve for prototype concrete. Possible exceptions are the gypsum concretes of higher  $f'_c$ , which appear to have stress-strain curves that are slightly closer to being linear than are the curves for prototype concrete.

#### Effect of Specimen Size on Strength

**Compressive Strength.** When compression tests are conducted on microconcrete cylinders of various sizes, the indicated compressive strength has sometimes been observed to increase with decreasing size of test cylinder.<sup>4,5</sup> At other times, no definite effect of cylinder size on compressive strength has been found.<sup>3,19</sup>

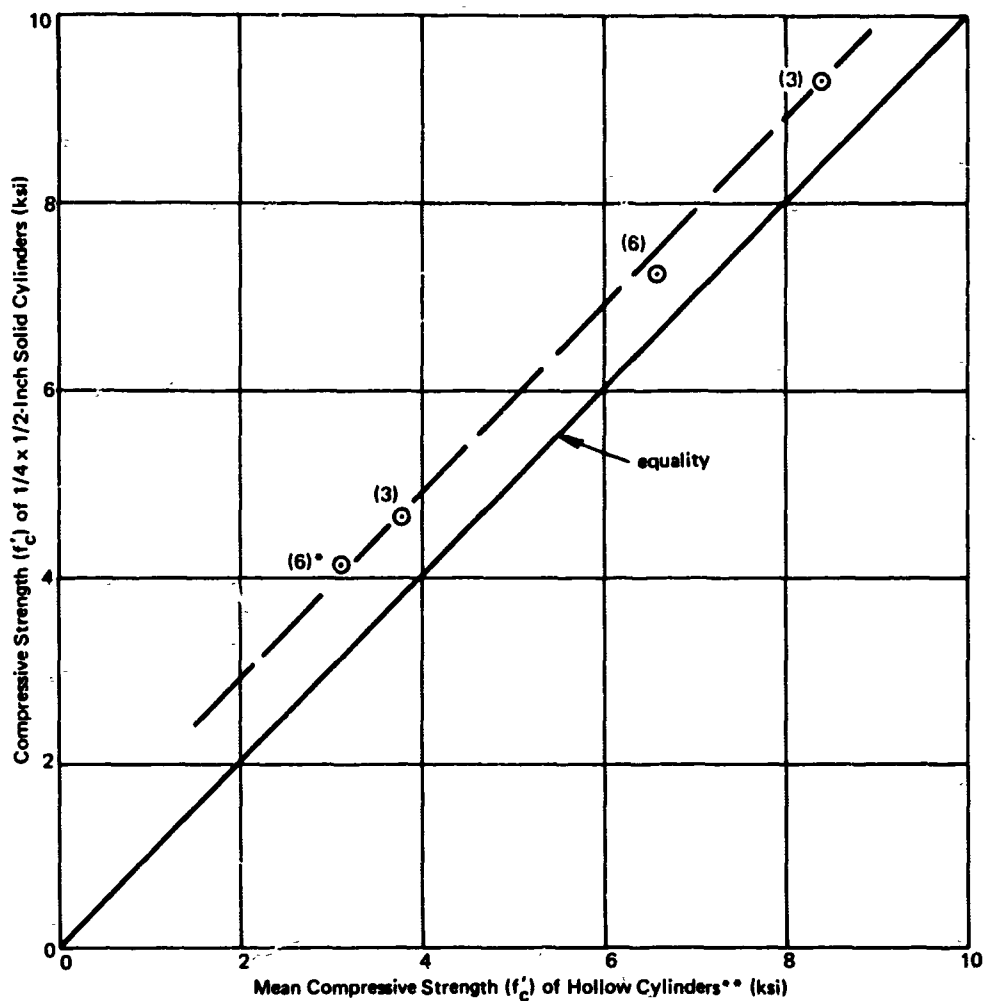
The approach adopted at the initiation of this investigation for choosing the size of test cylinder required the use of 1/4 x 1/2-inch solid cylinders for the model concretes containing No. 30 aggregate. For reasons mentioned earlier, hollow cylinders were used during most of the investigation in lieu of the 1/4 x 1/2-inch size solid cylinders.

A limited number of tests were performed in an attempt to correlate results from hollow cylinders with results from 1/4 x 1/2-inch solid cylinders. In the first such investigation, 1/4-inch-diameter solid cylinders and three sizes of hollow cylinders were cast from microconcrete having water-cement ratios of 0.5 and 0.9. The results from compression tests on these cylinders are presented in Table 7, where it can be seen that the size of hollow cylinders had no significant effect on  $f'_c$ .

Later in the investigation, additional data were sought on the correlation between results from cylinders of different sizes by testing microconcrete having water-cement ratios of 0.6 and 1.0. The results, shown in Table 7, indicated a large difference between the  $f'_c$  of the hollow cylinders and that of the 1/4 x 1/2-inch solid cylinders. From Table 7, then, there appears to be no consistent relationship between the strengths of hollow cylinders and those of 1/4 x 1/2-inch solid cylinders. However, when the results from the 1/4 x 1/2-inch solid cylinders of a given water-cement ratio are plotted versus the mean strength of hollow cylinders of the same water-cement ratio as taken from Figure 15, a more consistent relationship is evident. This is illustrated by Figure 32, where it can be seen that a straight line can be used to express the relationship between the  $f'_c$  of the different cylinders. This line indicates that for a wide range of  $f'_c$ , the compressive strength of 1/4 x 1/2-inch solid cylinders is about 900 psi greater than the strength of hollow cylinders. In designing a mix, it is proposed to provide for this 900-psi difference, as will be explained later.

When microconcrete having a water-cement ratio of 1.0 was tested in hollow cylinders and in 1 x 2-inch solid cylinders, there was no difference in the compressive strengths (Table 7). Subject to confirmation at other water-cement ratios, it appears that 1 x 2-inch solid cylinders as well as hollow cylinders can be used to determine  $f'_c$  for microconcrete containing No. 30 aggregate.

For gypsum concrete containing No. 30 aggregate, the effect of cylinder size on  $f'_c$  does not appear to be as large as that exhibited by microconcrete. For a water-cement ratio of 0.28, the average  $f'_c$  from six 1/4 x 1/2-inch solid cylinders was 4,720 psi, compared to 4,300 psi (Figure 15) for hollow cylinders. This is consistent with previous results,<sup>3</sup> where cylinder size was found to have little effect on the  $f'_c$  of sealed gypsum concrete. In mix design, it is proposed to assume that  $f'_c$  is independent of cylinder size for the gypsum concretes.



- \* Number in parentheses indicates the size of the test sample.
- \*\* From Figure 15.

Figure 32. Correlation between compressive strengths from different sized cylinders for microconcrete containing No. 30 aggregate.

Table 7. Effect of Cylinder Size and Water-Cement Ratio on Compressive Strength of Microconcrete Containing No. 30 Aggregate

Cylinder Size (in.)	Water-Cement Ratio			
	0.5	0.6	0.9	1.0
	Compressive Strength, $f'_c$ (psi)			
3/4 (OD) x 3/8 (ID) x 1-1/2	10,080	—	3,990	—
1 (OD) x 5/8 (ID) x 2	9,910	6,010	4,290	2,670
1 (OD) x 1/2 (ID) x 2	9,770	—	4,150	—
1/4 x 1/2	9,330	7,260 <sup>1/</sup>	4,670	4,160 <sup>1/</sup>
1 x 2	—	—	—	2,680

<sup>1/</sup> Average of six cylinders. Other results are average of three cylinders.

**Flexural Strength.** The flexural strengths of the model concretes containing No. 4 aggregate were determined from tests on 1-1/2 x 1-1/2 x 4-1/2-inch beams, scaled from the standard ASTM beam, and 1-1/2 x 3 x 9-inch beams. It was noted previously that for microconcrete the results from the smaller beams correlated better with the flexural strength of prototype concrete than did the results from the larger beams. Because of this, and because the dimensions of the smaller beams are derived from a scaling of the standard beam, the  $f'_f$  for model concretes should be determined from tests on the smaller beams. However, the larger beams are considerably easier to set up for testing. If it is desired to capitalize on this advantage, the values for  $f'_f$  from the larger beams can be correlated with the values for  $f'_f$  from the smaller beams by means of the curves shown in Figure 33. These curves indicate that the  $f'_f$  of the larger beams is about 84% and 94% of the  $f'_f$  of the smaller beams for microconcrete and gypsum concrete, respectively.

## MIX DESIGN PROCEDURE AND EXAMPLES

### Design Procedure

Before designing a mix, one must know the dimensions of the model and the desired type (microconcrete or gypsum concrete) and compressive strength of the model concrete as well as the volume of concrete required.

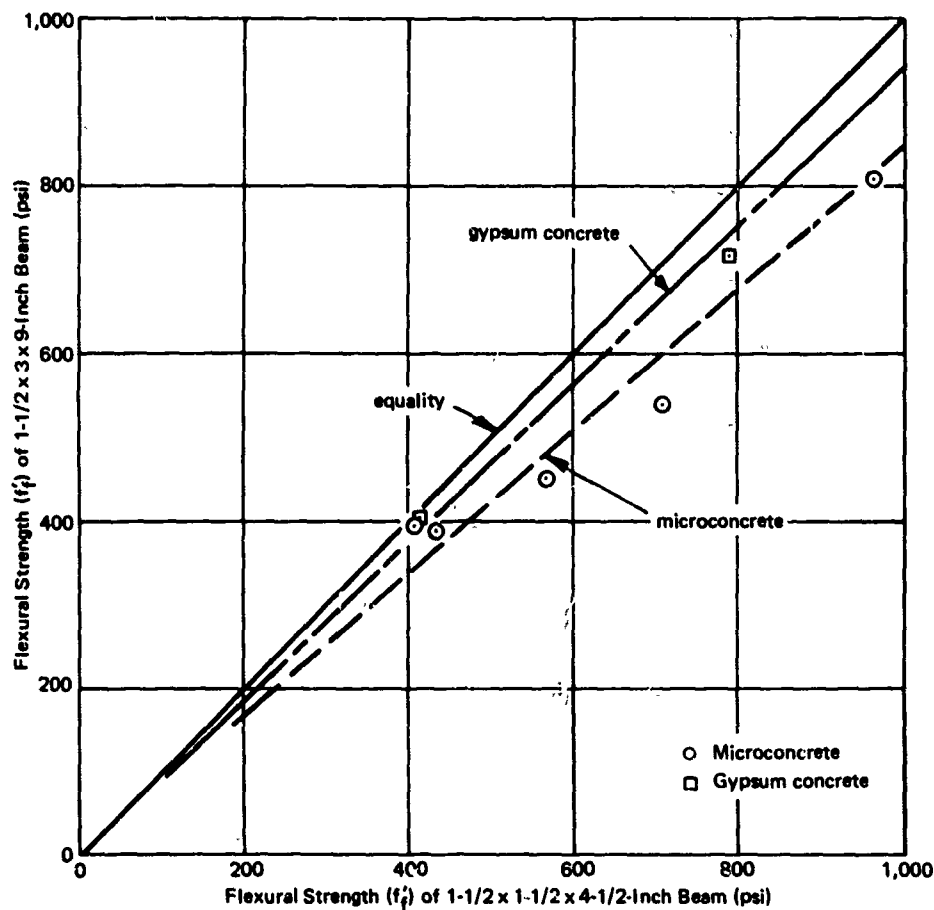


Figure 33. Correlation between flexural strengths from different sized beams for model concretes containing No. 4 aggregate.

Then, the aggregate and test specimen sizes, as well as the age for testing, are found in Table 8. Next, the required water-cement ratio is found in Figure 34, after which the aggregate-cement ratio is chosen from Figure 35. Finally, the weight of cement is determined from Figure 36.

In constructing the graph in Figure 34, the  $f'_c$  versus water-cement ratio curves for microconcrete containing No. 4 and No. 30 aggregate (Figures 14 and 15) were averaged, as were the corresponding curves for gypsum concrete, because of the small difference between the curves for the two aggregate sizes. For gypsum concrete and for microconcrete containing No. 4 aggregate, Figure 34 can be entered with the desired  $f'_c$  to find the correct water-cement ratio. For microconcretes containing aggregate sizes other than No. 4, the desired  $f'_c$  must be adjusted before entering Figure 34. This adjustment arises because, for No. 30 aggregate, the hollow and the

1/4 x 1/2-inch cylinders differed in  $f'_c$  by 900 psi (Figure 32). Therefore, to maintain consistency in the approach to mix design, 900 psi should be subtracted from the desired  $f'_c$  before entering Figure 34. To interpolate between No. 30 and No. 4 aggregate, 600 and 300 psi should be subtracted from the desired  $f'_c$  for microconcrete containing No. 16 and No. 8 aggregate, respectively. No tests have been conducted to check the validity of the interpolation procedure.

For microconcrete models to be tested at the ages shown in Table 8, but to be subjected to other than 2 days of drying, the desired  $f'_c$  should be adjusted as indicated by the results shown in Figure 17 before entering Figure 34 to find the water-cement ratio.

Table 8. Model Characteristics

Typical Dimension in Model <sup>1/</sup> (in.)	Maximum Aggregate Size	Cylinder Size <sup>2/</sup> (in.)	Beam Size <sup>3/</sup> (in.)	Age at Testing (days)	
				Micro-concrete <sup>4/</sup>	Gypsum Concrete <sup>5/</sup>
3	3/8 in.	3 x 6	3 x 3 x 9	24	2
1-1/2	No. 4	1-1/2 x 3	1-1/2 x 1-1/2 x 4-1/2	18	2
3/4	No. 8	3/4 x 1-1/2	3/4 x 3/4 x 2-1/4 <sup>6/</sup>	15	2
1/2	No. 16	1/2 x 1 <sup>6/</sup>	1/2 x 1/2 x 1-1/2 <sup>6/</sup>	14	2
1/4	No. 30	1 (OD) x 5/8 (ID) x 2 <sup>7/</sup>	- <sup>7/</sup>	13	2

<sup>1/</sup> Width or depth of beam or column, or thickness of slab or shell.

<sup>2/</sup> Used in determining  $f'_c$  and  $f'_{sp}$ .

<sup>3/</sup> Used in determining  $f'_t$ .

<sup>4/</sup> Cure in 100% RH until 2 days before test, then store in controlled laboratory environment.

<sup>5/</sup> Seal with shellac at an age of about 2 hours; cure in laboratory environment.

<sup>6/</sup> Tests have not been performed on specimens of these sizes, but it is believed that such tests would not be unduly difficult.

<sup>7/</sup> The indication of  $f'_t$  normally provided by  $f'_{sp}$  or  $f'_t$  can be obtained from splitting tensile strength tests on 1 x 2-inch cylinders or, for gypsum concrete, possibly from flexural strength tests on hollow beams.

## Mix Design Examples

### Gypsum Concrete

- Given: 1. Gypsum concrete model with 1-1/2-in.<sup>2</sup> columns  
 2.  $f'_c = 3,500$  psi  
 3. 300 in.<sup>3</sup> of concrete required.

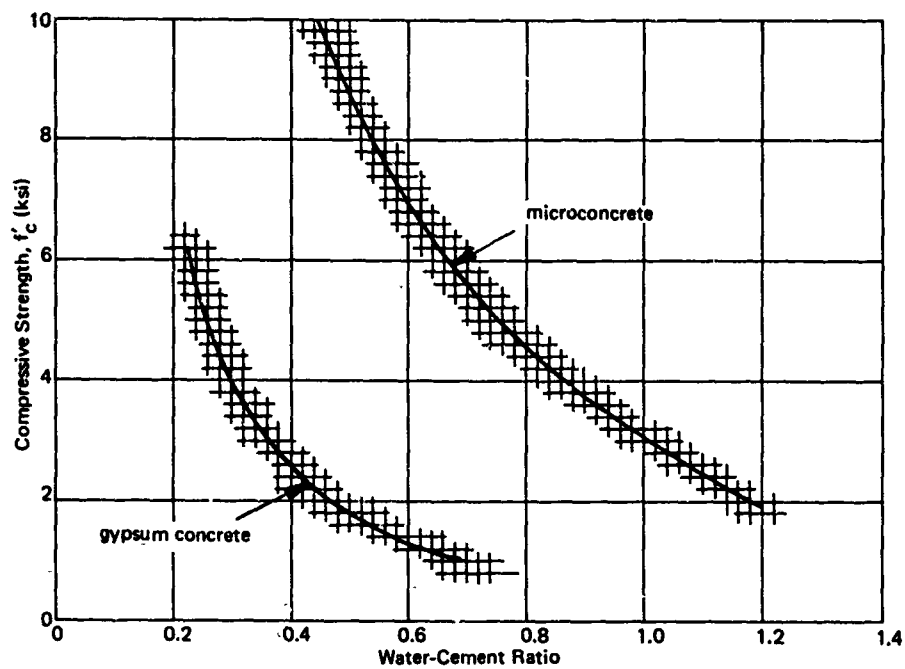


Figure 34. Compressive strength versus water-cement ratio for model concretes.

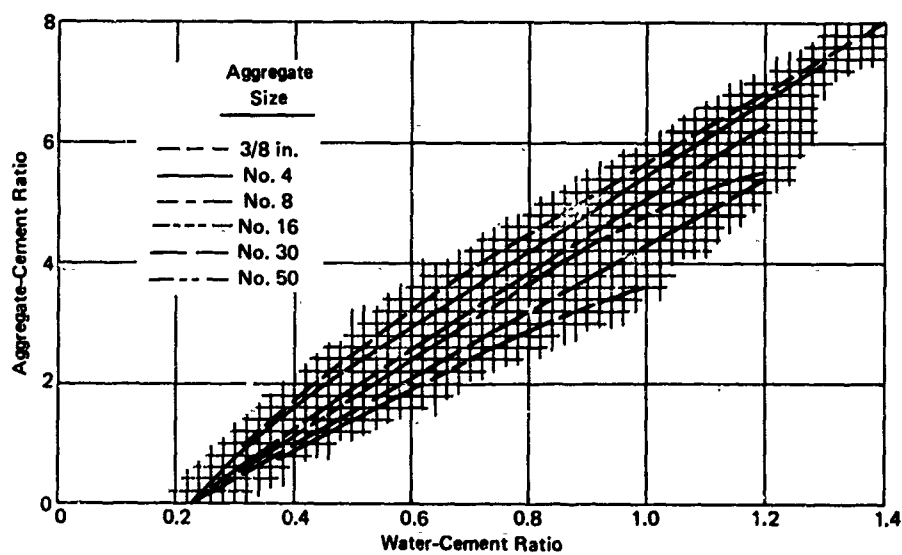


Figure 35. Workability curves for concretes containing aggregates of various sizes.

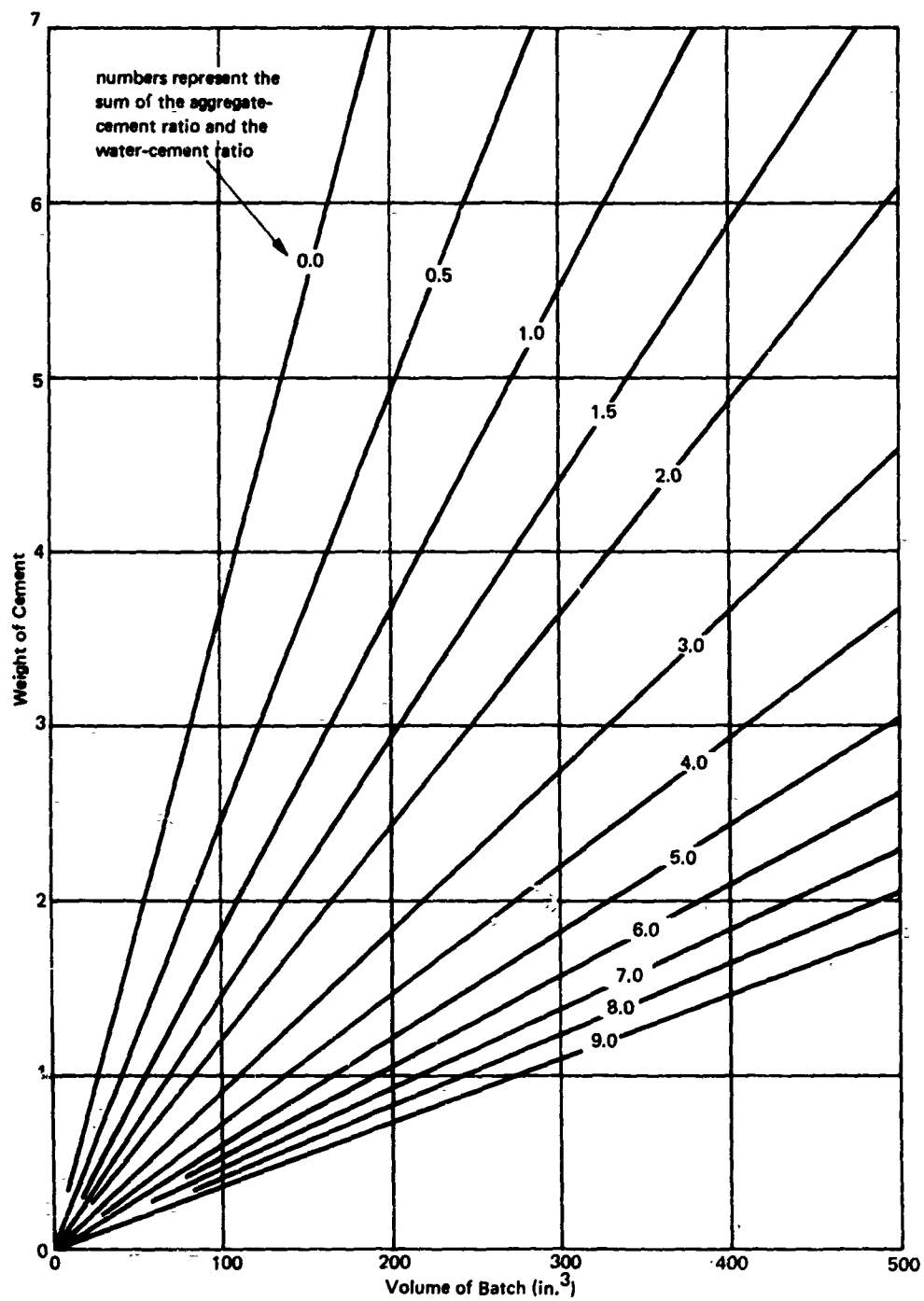


Figure 36. Weight of cement versus volume of batch for various aggregate-cement and water-cement ratios.

Step 4. Enter Figure 34.

Water-cement ratio = 0.78

Step 5. Enter Figure 35.

Aggregate-cement ratio = 3.70

Step 6. Enter Figure 36.

Cement  $\approx$  700 gm

Step 7. Compute water and aggregate.

Water =  $0.78 \times 700 = 546$  gm

Aggregate =  $3.70 \times 700 = 2,590$  gm

#### Microconcrete With Drying-Time Adjustment

- Given:
1. Microconcrete model with 0.2-inch-thick slab
  2.  $f'_c = 3,000$  psi
  3. 150 in.<sup>3</sup> of concrete required
  4. Model to be dried for less than 2 hours before testing

Step 1. Enter Table 8.

Aggregate Size = No. 30

Cylinder Size = 1 (OD)  $\times$  5/8 (ID)  $\times$  2 in.

Age at Testing = 13 days

Step 2. Adjust size of cylinder and aggregate to  $f'_c$ .

Adjustment = 900 psi (see text above)

Adjusted  $f'_c = 3,000 - 900 = 2,100$  psi

Step 3. Adjust drying time to  $f'_c$  (Figure 17):

Adjustment Factor = 0.81

Adjusted  $f'_c = 2,100/0.81 \approx 2,600$  psi

Step 4. Enter Figure 34.

Water-cement ratio = 1.08

Step 5. Enter Figure 35.

Aggregate-cement ratio = 4.75

Step 6. Enter Figure 36.

Cement  $\approx$  800 gm

Step 7. Compute water and aggregate.

Water =  $1.08 \times 800 = 864$  gm

Aggregate =  $4.75 \times 800 = 3,800$  gm

Step 4. Enter Figure 34.

Water-cement ratio = 0.78

Step 5. Enter Figure 35.

Aggregate-cement ratio = 3.70

Step 6. Enter Figure 36.

Cement  $\approx$  700 gm

Step 7. Compute water and aggregate.

Water =  $0.78 \times 700 = 546$  gm

Aggregate =  $3.70 \times 700 = 2,590$  gm

#### Microconcrete With Drying-Time Adjustment

Given: 1. Microconcrete model with 0.2-inch-thick slab

2.  $f'_c = 3,000$  psi

3. 150 in.<sup>3</sup> of concrete required

4. Model to be dried for less than 2 hours before testing

Step 1. Enter Table 8.

Aggregate Size = No. 30

Cylinder Size = 1 (OD)  $\times$  5/8 (ID)  $\times$  2 in.

Age at Testing = 13 days

Step 2. Adjust size of cylinder and aggregate to  $f'_c$ .

Adjustment = 900 psi (see text above)

Adjusted  $f'_c = 3,000 - 900 = 2,100$  psi

Step 3. Adjust drying time to  $f'_c$  (Figure 17).

Adjustment Factor = 0.81

Adjusted  $f'_c = 2,100/0.81 \approx 2,600$  psi

Step 4. Enter Figure 34.

Water-cement ratio = 1.08

Step 5. Enter Figure 35.

Aggregate-cement ratio = 4.75

Step 6. Enter Figure 36.

Cement  $\approx$  800 gm

Step 7. Compute water and aggregate.

Water =  $1.08 \times 800 = 864$  gm

Aggregate =  $4.75 \times 800 = 3,800$  gm

## EVALUATION OF MIX DESIGN PROCEDURE

The data for mix design (Figures 17, 32, 34, and 35) were gathered under a given set of casting, curing, and testing techniques and aggregate from a single source and cement from a single manufacturer were used. The casting, curing, and testing techniques are repeatable, or very nearly so, by others interested in using the mix design data. However, others will not be able, in general, to use cements and aggregate from the sources used in developing the data. How will this effect the strength and workability of model concretes (see Table 9) designed on the basis of the reported data?

It is likely that the workability (Figure 35) will be little affected by the source of materials, providing the aggregate is processed and recombined into the gradations shown in Table 3 and has a moisture content of about 0.3% (or a suitable correction to the amount of water added is made for aggregates having other moisture contents). The strength data (Figure 34) are likely to be more sensitive to the source of materials. For example, it is well known that cements from different manufacturers, or even cements from the same manufacturer but made at different times, sometimes produce concretes of decidedly different strengths. Therefore, if the  $f'_c$  of the concrete in a model is critical, that is, if the  $f'_c$  specified in mix design must be obtained within a few percent, a trial batch of model concrete should be prepared and its strength determined. If the strength is not as desired, trial batches of other water-cement ratios (and aggregate-cement ratios from Figure 35) can be prepared, using Figure 34 for guidance in choosing the water-cement ratio until a mix of the desired  $f'_c$  is obtained.

It seems particularly important that trial batches be made and tested when cylinder- and aggregate-size and drying-time adjustments (Steps 2 and 3 in the mix design procedure) are used in the mix design. These adjustments are based on a very limited amount of experimental data (Figures 17 and 32), and the interpolation procedure for adjusting cylinder and aggregate size to microconcrete containing No. 8 and No. 16 aggregate has not been checked by tests.

Another question likely to arise concerns the validity of the approach for choosing the size of test cylinder to be used with a particular model. This question can be answered only after a number of models of structural elements, wherein the ultimate strength is highly dependent on  $f'_c$ , have been tested and the results scaled to a full-sized element and compared with the results of tests on the full-sized element. This constitutes one of the goals of future work in modeling at NCEL.

Similarly, a question might arise concerning the effects on the predictions from model tests of the observed differences in the mechanical properties of model and prototype concretes of the same compressive strength.

In some model tests, it is possible to partially compensate for the differences in the compressive stress-strain curve properties by using distorted models of the prototype.<sup>3</sup> When true models are used, however, the fact that the modulus of elasticity for model concrete is lower than the modulus for prototype concrete will generally result in deflections predicted from model tests that are too large relative to the actual deflections of the prototype. With the exception of the modulus of elasticity, the differences between the properties of model and prototype concretes are fairly small. Any significant effects of these differences can be best detected by testing models of various structural elements, scaling the model results to prototype size, and comparing the scaled results with the results from tests on the prototype. This use of scaling is another of the goals of future work in modeling at NCEL.

Table 9. Comparison of Characteristics of Microconcrete and Gypsum Concrete

Characteristic <sup>1/</sup>	Microconcrete		Gypsum Concrete	
	No. 4 Aggregate	No. 30 Aggregate	No. 4 Aggregate	No. 30 Aggregate
Splitting tensile strength	essentially the same	essentially the same for high water-cement ratios; slightly high for low water-cement ratios	slightly low	essentially the same
Flexural strength	essentially the same	—	essentially the same	—
Initial tangent modulus	low	low	low	low
Ultimate strain	high	high	slightly high	essentially the same
Shape of stress-strain curve	slightly more curvature	slightly more curvature	essentially the same for high water-cement ratios; slightly less curvature for low water-cement ratios	less curvature

<sup>1/</sup> Model concrete compared to prototype concrete.

## CONCLUSIONS

1. The mix design procedure developed for model concretes is easy to apply, and can be used to produce model concretes having compressive strengths ranging from 1,000 to more than 10,000 psi. Model concretes designed in accordance with the procedure can be expected to have adequate workability. Generally, tests on a few model concretes of different water-cement ratios will be necessary to define the ratios producing a concrete of the desired compressive strength.
2. Compared to a prototype concrete of the same compressive strength, a model concrete designed by the procedure presented and cast, cured, and tested by the techniques used in collecting the mix design data, will have characteristics shown in Table 9.
3. Hollow cylinders can be used in lieu of 1/4 x 1/2-inch cylinders for determining the compressive strength of model concretes containing No. 30 aggregate; the hollow cylinders are easier to cast, cap, and test.
4. For both microconcrete and gypsum concrete, at a particular water-cement ratio, the compressive strength of concrete containing No. 4 aggregate tested in 1-1/2 x 3-inch cylinders can be expected to be about the same as the compressive strength of concrete containing No. 30 aggregate tested in 1 (OD) x 5/8 (ID) x 2-inch hollow cylinders.
5. The forming, casting, capping, and testing techniques used in this investigation produced satisfactory specimens and results and can be used to facilitate future investigations of the properties or behavior of small test specimens.
6. Subject to further experimental confirmation, flexural tests on hollow beams can be used to gain an indication of the tensile strength of thin layers of gypsum concrete.

## ACKNOWLEDGMENTS

Mr. D. S. Harrington, formerly Engineering Technician, NCEL, was responsible for the design of forms and special equipment, the manufacture and testing of all specimens, the reduction of test data, and the preparation of the first draft of the section of the report on experimental techniques. His many contributions to the successful accomplishment of the work are gratefully acknowledged.

Mr. R. A. Breckenridge, Research Structural Engineer, NCEL, and Dr. H. I. Laursen, Associate Professor of Civil Engineering, Oregon State University, participated in the planning of the work. Mr. G. M. Dunn, Engineer-in-Training, NCEL, assisted with part of the testing program and the collection of splitting tensile strength data on prototype concrete. Mr. I. W. Anders, Mathematician, NCEL, performed the regression analyses of the splitting tensile strength data.

## Appendix

### COMPARISON OF ULTRACAL 30 AND HYDRO-STONE AS CEMENTING AGENTS FOR GYPSUM CONCRETE

Data furnished by the manufacturer on the strength of Hydro-stone-water mixtures suggested that for a given water-cement ratio or aggregate-cement ratio Hydro-stone-based gypsum concretes might have a higher compressive strength ( $f'_c$ ) than Ultracal 30-based gypsum concretes. If so, the range of application for gypsum concretes could be extended to include the modeling of structures composed of high-strength concretes.

A limited number of tests were performed to determine the differences, if any, in the strength properties of Ultracal 30- and Hydro-stone-based gypsum concretes having No. 4 aggregate and a water-cement ratio of 0.325. The results of the tests are shown in Figure 37 and Table 10.

Table 10. Comparison of Strength Properties of Ultracal 30- and  
Hydro-stone-Based Gypsum Concrete Containing No. 4  
Aggregate, Water-Cement Ratio = 0.325

Property	Age 4 hr		Age 2 days		Age 8 days	Age 10 days
	Ultracal 30	Hydro-stone	Ultracal 30	Hydro-stone	Ultracal 30	Hydro-stone
$f'_c$ (psi)	3,530	3,720	3,510	3,580	3,260	3,620
$f'_{sp}$ (psi)	—	—	257	262	—	—
$E_c$ (psi $\times 10^6$ )	—	—	2.45	2.03	2.46	2.18
$E_{sec}^{1/}$ (psi $\times 10^6$ )	—	—	2.09	1.70	2.07	1.71
$\epsilon_o$ (in./in.)	—	—	2,600	3,070	2,610	3,480

<sup>1/</sup> To 50%  $f'_c$ .

Figure 37 shows that the relationships between  $f'_c$  and age in both the sealed and unsealed conditions are similar for the two types of gypsum concrete. For a given age and sealing condition,  $f'_c$  for the Hydro-stone concrete was always slightly greater than for the Ultracal 30 concrete. The only notable difference in the relationships between  $f'_c$  and age occurred at an age of more than 2 days, when the  $f'_c$  of the sealed Ultracal 30 specimens decreased while  $f'_c$  of the sealed Hydro-stone specimens remained constant.

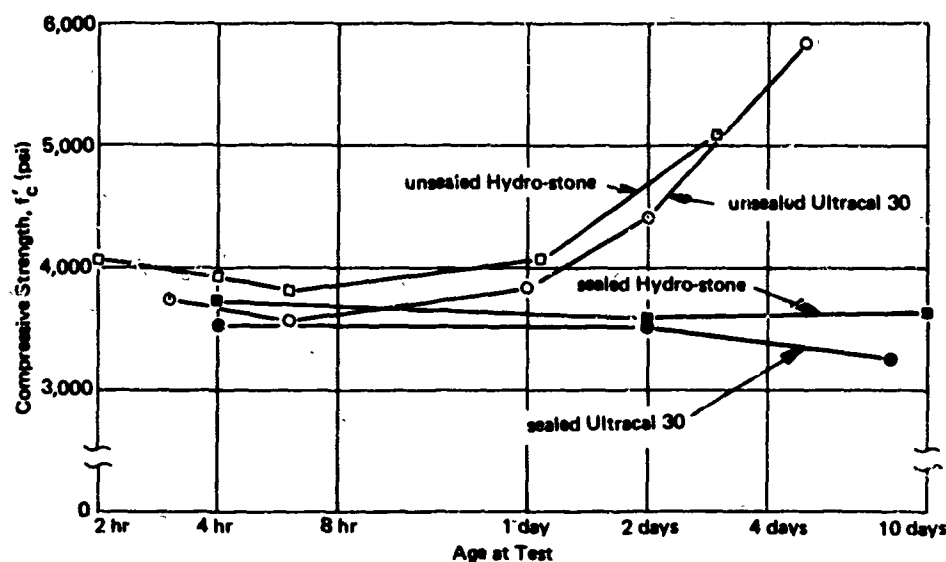


Figure 37. Comparison of compressive strength-age relation for 1-1/2 x 3-inch cylinders made from Ultracal 30 and Hydro-stone gypsum concretes containing No. 4 aggregate (water-cement ratio = 0.325).

The results in Table 10 indicate that the splitting tensile strength was essentially the same for the two types of gypsum concrete when sealed. However, the characteristics of the compressive stress-strain curve differed for the two types; at a given age, the Ultracal 30 concretes showed a greater initial tangent modulus of elasticity and less strain at maximum stress. This means that an Ultracal 30 concrete of a certain  $f'_c$  would provide a better representation of the stress-strain curve of prototype concrete of the same  $f'_c$  than would Hydro-stone concrete (see Figure 28). Although  $f'_c$  for the Ultracal 30 concrete decreased between the ages of 2 and 8 days, it is interesting to note from Table 10 that the characteristics of the stress-strain curve remained unchanged.

Ultracal 30 was used as the cementing agent in all the gypsum concretes for which results are presented in the preceding sections of this report. Ultracal 30 was chosen over Hydro-stone because, as discussed above, it appears to provide a better representation of the prototype concrete stress-strain curve. Another factor in the choice was the difficulty encountered in capping the Hydro-stone concrete cylinders; the capping material did not adhere well to the slick surface of the cylinders.

Because of the small difference in  $f'_c$  at an age of 2 days (Table 10), it is likely that the curve for  $f'_c$  versus water-cement ratio for gypsum concrete (Figure 34) can be used for the mix design of Hydro-stone-based concretes, as well as for Ultracal 30-based concretes, should it be desired to use Hydro-stone as the cementing agent.

## LIST OF SYMBOLS

$a$	Coefficient of $f'_c$ in Equation 2
$b$	Pure constant in Equation 2, psi
$d$	Diameter of cylinder or wall thickness of hollow cylinder, in.
$E_c$	Initial tangent modulus of elasticity of concrete in compression, psi
$E_{sec}$	Secant modulus of elasticity of concrete in compression, psi
$f_c$	Compressive stress, psi
$f'_c$	Compressive strength of concrete, psi
$f'_f$	Flexural strength of concrete, psi
$f'_{sp}$	Splitting tensile strength of concrete, psi
$f'_t$	Direct tensile strength of concrete, psi
$m$	Exponent of $f'_c$ in Equation 2
$\epsilon$	Compressive strain, $\mu\text{in./in.}$
$\epsilon_o$	Strain at maximum compressive stress, $\mu\text{in./in.}$

## REFERENCES

1. Cornell University. School of Civil Engineering. Report no. 325: A bibliography on structural analysis (with particular emphasis on concrete structures), by G. M. Sabnis and R. N. White. Ithaca, N. Y., Sept. 1966.
2. R. N. White. "Small-scale models of concrete structures," paper presented at American Society of Civil Engineers Structural Engineering Conference and annual meeting, New York, Oct. 19-23, 1964. (ASCE preprint 131)
3. Cornell University. School of Civil Engineering. Report no. 326: Small scale direct models of reinforced and prestressed concrete structures, by H. G. Harris, G. M. Sabnis, and R. N. White. Ithaca, N. Y., Sept. 1966. (National Science Foundation Grant GP-2622)
4. Massachusetts Institute of Technology. Department of Civil Engineering. Report R63-54: Techniques and materials in the modeling of reinforced concrete structures under dynamic loads, by H. G. Harris, et al. Cambridge, Mass., Dec. 1963. (Contract NBy-32228) (AD 602034)
5. R. P. Johnson. "Strength tests on scaled-down concretes suitable for models, with a note on mix design," Magazine of Concrete Research, vol. 14, no. 40, Mar. 1962, pp. 47-53.
6. U. S. Naval Civil Engineering Laboratory. Technical Note N-236: Investigation of West Coast aggregates, by U. W. Stoll. Port Hueneme, Calif., Dec. 1955.
7. \_\_\_\_\_. Technical Report R-447: Dynamic properties of plain portland cement concrete, by W. L. Cowell. Port Hueneme, Calif., June 1966. (AD 635055)
8. W. E. Grieb and G. Werner. "Comparison of the splitting tensile strength of concrete with flexural and compressive strengths," Public Roads, vol. 32, no. 5, Dec. 1962, pp. 97-106.
9. U. S. Naval Civil Engineering Laboratory. Technical Report R-395: Dynamic shear strength of reinforced concrete beams — Part I, by W. A. Keenan. Port Hueneme, Calif., Dec. 1965. (AD 627661)
10. J. A. Hanson. "Tensile strength and diagonal tension resistance of structural-lightweight concrete," American Concrete Institute, Journal, Proceedings, vol. 58, no. 1, July 1961, pp. 1-40.
11. U. S. Naval Civil Engineering Laboratory. Technical Report R-502: Dynamic shear strength of reinforced concrete beams — Part II, by R. H. Seabold. Port Hueneme, Calif., Jan. 1967. (AD 644823)

12. M. S. E. B. Nosseir. Static and dynamic behavior of concrete beams failing in shear, Ph D thesis, University of Texas. Austin, Tex., June 1966.
13. B. B. Broms. "Crack width and crack spacing in reinforced concrete members, part 1," American Concrete Institute, Journal, Proceedings, vol. 62, no. 10, Oct. 1965, pp. 1237-1256. (Part 2 supplement contains details on test techniques, procedures, and test data, published separately. Detroit, Mich., American Concrete Institute, 1965.)
14. B. B. Broms and L. A. Lutz. "Effects of arrangement of reinforcement on crack width and spacing of reinforced concrete members, part 1," American Concrete Institute, Journal, Proceedings, vol. 62, no. 11, Nov. 1965, pp. 1395-1410. (Part 2 supplement contains details on test techniques, procedures, and test data, published separately. Detroit, Mich., American Concrete Institute, 1965.)
15. I. Narrow and E. Ullberg. "Correlation between tensile splitting strength and flexural strength of concrete," American Concrete Institute, Journal, Proceedings, vol. 60, no. 1, Jan. 1963, pp. 27-37.
16. H. F. Gonnerman and E. C. Shuman. "Compression, flexure, and tension tests of plain concrete," American Society for Testing and Materials, Proceedings, vol. 28, pt. 2, 1928, pp. 527-552.
17. University of Illinois. Engineering Experiment Station. Bulletin no. 399: A study of combined bending and axial load in reinforced concrete members, by E. Hognestad. Urbana, Ill., Nov. 1951.
18. E. Hognestad, N. W. Hanson, and D. McHenry. "Concrete stress distribution in ultimate strength design," American Concrete Institute, Journal, Proceedings, vol. 52, no. 4, Dec. 1955, pp. 455-479.
19. W. A. Litle and M. Paparoni. "Size effect in small-scale models of reinforced concrete beams," American Concrete Institute, Journal, Proceedings, vol. 63, no. 11, Nov. 1966, pp. 1191-1204.

Unclassified

Security Classification

DOCUMENT CONTROL DATA - R & D		
<i>(Security classification of title, body of abstract and indexing annotation must be entered when the overall report is classified)</i>		
1. ORIGINATING ACTIVITY (Corporate author) Naval Civil Engineering Laboratory Port Hueneme, California 93C41		2a. REPORT SECURITY CLASSIFICATION Unclassified
		2b. GROUP
3. REPORT TITLE  MIX DESIGN FOR SMALL-SCALE MODELS OF CONCRETE STRUCTURES		
4. DESCRIPTIVE NOTES (Type of report and inclusive dates) Not final; January 1966 to March 1967		
5. AUTHOR(S) (First name, middle initial, last name)  D. S. Fuss		
6. REPORT DATE February 1968	7a. TOTAL NO. OF PAGES 66	7b. NO. OF REFS 19
8a. CONTRACT OR GRANT NO. DASA-RSS3318	8b. ORIGINATOR'S REPORT NUMBER(S)  TR-564	
b. PROJECT NO. Y-F008-08-02-126		
c.	9b. OTHER REPORT NO(S) (Any other numbers that may be assigned this report)	
d.		
10. DISTRIBUTION STATEMENT This document has been approved for public release and sale; its distribution is unlimited. Copies available at the Clearinghouse for Federal Scientific & Technical Information (CFSTI), Sills Building, 5285 Port Royal Road, Springfield, Va, 22151 Price-\$3.00		
11. SUPPLEMENTARY NOTES		12. SPONSORING MILITARY ACTIVITY  Naval Facilities Engineering Command Washington, D. C.
13. ABSTRACT <p>An easily applied method of mix design was developed for concretes suitable for use in small-scale models of concrete structures. By use of the method, model concretes of adequate workability can be produced having compressive strengths ranging from 1,000 to more than 10,000 psi.</p> <p>Data on mechanical properties were collected for model concretes with portland cement and gypsum cement bases. These concretes had maximum aggregate sizes of No. 4 (suitable for many model beams and columns) and No. 30 (suitable for model slabs and shells). Compared to prototype concretes of equal compressive strength, the model concretes using approximately scaled aggregate were found to have about the same splitting-tensile strength and flexural strength, a lower elastic modulus in compression, and, generally, a higher strain at maximum compressive stress.</p> <p>Described in the report are techniques for the manufacture and testing of small concrete specimens. Information is given on the size of test specimen to use with a particular model as well as on the age for testing the specimen and model.</p>		

DD FORM 1473

1 NOV 65

(PAGE 1)

S/N 0101-807-6001

Unclassified

Security Classification

Unclassified  
Security Classification

14	KEY WORDS	LINK A		LINK B		LINK C	
		ROLE	WT	ROLE	WT	ROLE	WT
	Concrete						
	Concrete mixes						
	Concrete mix design						
	Microconcrete						
	Gypsum concrete						
	Small-scale models						
	Compressive strength tests						
	Flexural strength tests						
	Direct tensile strength tests						
	Splitting tensile strength tests						
	Test cylinders						
	Hollow test cylinders						
	Test beams						
	Hollow test beams						